Studies of exosome dynamics in mice and canines during normal pregnancy and the roles of exosomes and microRNA in the pathogenesis of preeclampsia

マウスとイヌの正常妊娠期におけるエクソソームの動態、および妊娠高血圧症候群モデルにおけるエクソソームとマイクロRNAの役割

Joint Graduate School of Veterinary Medicine

Yamaguchi University

LITA RAKHMA YUSTINASARI

September, 2024

DECLARATION

I hereby declare that the work reported in this research project report has been carried out by the undersigned. I also declare that where reference has been made to the results of other workers, appropriate acknowledgment of the source of information has been made.

September, 2024 Yamaguchi University Author

Lita Rakhma Yustinasari

ACKNOWLEDGMENT

First of all, all praise goes to **Allah** جل جلاله for His gracious guidance that enabled to complete my research and through all the difficulties in my life.

I am grateful to have had **Prof. Dr. Ken Takeshi KUSAKABE** as my main supervisor during my Ph.D. studies in Veterinary Anatomy for his wholehearted guidance, advice, and inspiration not only in academics but also in my personal life. He gave me the opportunity to be his student even after we met for the first time during my short course program at Yamaguchi University. I could never have learned advanced immunohistochemical and molecular biological techniques, as well as reviewing and writing scientific papers, without his assistance. He always showed patience and never spoke with a high tone, even when I faced troubles while performing research experiments. I cannot express enough gratitude for his support during my four-year life in Japan. Thank you very much, Professor Kusakabe.

It is my pleasure to express my sincere gratitude to **Dr. Hiroyuki IMAI** for his patience and tireless tutoring during my first time in the laboratory. Without his support, I probably would not have been able to carry out my experiments as quickly and accurately as I can now. I learned a lot from him, not just the techniques but also the way to organize experiments and the standard behavior for avoiding material contamination.

I would like to gratefully acknowledge other members of the supervisory committee **Prof. Dr. Kiyoshi KANO**, **Prof. Dr. Akikazu FUJITA, Prof. Dr. Masahiro MORIMOTO**, and **Dr. Shusaku SHIBUTANI** who always supported during my study. Also, I am deeply grateful to **Prof. Dr. Hiroshi SATO**, who had introduced me to my main supervisor.

I would like to express my deep gratitude to all current and former students of Kusakabe sensei's laboratory for their assistance, technical support, and scientific collaboration during my research. Thankful to the staff members of the United Graduate School of Veterinary Science's office and International Support Center of Yamaguchi University for their

cooperation in preparing documents needed, as well as all staff member of i-COVER who helped me maintain the animal experiments during my research.

Special thanks appreciated to the Ministry of Education, Culture, Sports, Science and Technology (Monbukagakusho) of Japan for awarding me the scholarship that allowed me to pursue my studies and research at Yamaguchi University.

Grateful to Hirakawa-no-Kazeno Kai, all volunteers in the Nihongo class for children, the teachers at Hirakawa Elementary School, particularly Shinichiro Tsujimoto sensei, as well as all the members of Perhimpunan Pelajar Indonesia (PPI) Yamaguchi. Thanks to their support, my family's life has become enjoyable here.

I would like to thank Prof. Dr. Pudji Srianto, Prof. Dr. Fedik Abdul Rantam, Dr. Mufasirin, Chairul Anwar drh, Dr. Eka Pramyrtha Hestianah, Dr. Suryo Kuncorojakti, Prof. Dr. Widjiati, Prof. Epy Luqman, Dr. Soeharsono, and all my colleagues in the Faculty of Veterinary Medicine, Airlangga University, whom I could not mention individually.

I would like to express my sincere gratitude to my beloved parents Heri Triharyanto and Siti Rokhmi Fuadati, my brother Yuristo Ardi Hanggoro, my sister-in-law, Inggar Nur Amalia, and their cute children, Alula Kalani Pratista and Aidia Sasi Kirana. Their never-ending support has been crucial in helping me achieve the highest level of success in my study.

Last but not least, I would like to express the deepest thankfulness to my husband, Dr. Agus Widodo, for his patience, love, loyalty, and support throughout this time. I particularly appreciate him taking care of my mother while we were in a long-distance relationship. I am also grateful to my beloved daughter, Seira Mahira Azkadina, and son, Muhammad Rafiandra Maher El Shabaz, for their unconditional love and mature attitude in dealing with all situations, despite their young age. Without their support, the recent study would have been merely a distant dream.

Lita Rakhma Yustinasari

TABLE OF CONTENTS

DECLARATION ii
ACKNOWLEDGMENT iii
TABLE OF CONTENTS v
LIST OF TABLES viii
LIST OF FIGURES ix

GENERAL INTRODUCTION 1

OBJECTIVES 4

CHAPTER 1 5
1.1 Abstract 6
1.2 Introduction 6
1.3 Materials and Methods 8
1.3.1 Animal samples 8
1.3.2 Histological analysis 9
1.3.3 RNA isolation and RNA-Seq analyses 9
1.3.4 RT-PCR analysis 10
1.3.5 Western blot analysis 10
1.3.6 *Isolation of extracellular vesicles (EVs)* 11
1.3.7 Observation of EVs using transmission electron microscopy (TEM) 12
1.3.8 Cell-free RNA purification and real-time PCR analysis 12
1.3.9 Statistical analysis 12
1.4 Results 13
1.4.1 Histological observation 13
1.4.2 Gene expression of canine placentas by RNA-Seq and RT-PCR 13
1.4.3 Western blotting on canine pregnant serums 13
1.4.4 Analysis of exosomes in canine pregnant serum 14
1.4.5 Analyses of cell-free RNA in the serum 15
1.5 Discussions 16

CHAPTER 2 26
2.1 Abstract 27
2.2 Introduction 27
2.3 Materials and Methods 30
2.3.1 Laboratory animals 30
2.3.2 Isolation of extracellular vesicles (EVs) 30
2.3.3 Nanoparticle-tracking assay (NTA) 30
2.3.4 Transmission electron microscopy (TEM) 31
2.3.5 Immunohistochemistry (IHC) 31
2.3.6 *Western blot (WB)* 32
2.3.7 Detection of microRNA (miRNA) 33
2.3.8 Statistical analysis 34
2.4 Results 34
2.4.1 Dynamics of the exosomes in the pregnant serum 34
2.4.2 Western blots by tetraspanin markers and syncytin-1 36
2.4.3 Detection of exosomes in mouse placentas 36
2.4.4 Detection of miRNA in mouse serum-derived EVs 37
2.5 Discussions 37

CHAPTER 3 46
3.1 Abstract 47
3.2 Introduction 47
3.3 Materials and Methods 50
3.3.1 Laboratory animals 50
3.3.2 Isolation of extracellular vesicles (EVs) 51
3.3.4 Transmission electron microscopy (TEM) 51
3.3.5 Immunohistochemistry (IHC) 51
3.3.6 *Western blot (WB)* 52
3.3.7 Detection of microRNA (miRNA) by Real-Time PCR 53
3.3.8 Statistical analysis 54
3.4 Results 54
3.4.1 L-NAME administration to pregnant mice showed preeclampsia phenotypes ..54
3.4.2 Histopathological changing in preeclampsia mouse placenta 55
3.4.3 Dynamics of the exosomes in the serum of healthy pregnancy and preeclampsia 55

3.4.4 VEGF and iNOS protein expression after L-NAME administration 56
3.4.5 Detection of miRNA in mouse serum-derived EVs 56
3.5 Discussions 57

GENERAL DISCUSSION 66

REFERENCES 73

SUMMARY 86

LIST OF TABLES

Table 1.1 Highly expressed genes in the canine placentas at late pregnancy 14

Table 1.2 Measurements of extracellular vesicles (EVs) and exosomes in the canine serums ..15

Table 2.1 List of primary and secondary antibodies used in western blot and immunohistochemistry.....33

Table 2.2 Primer sequences for qPCR.....34

Table 2.3. Measurements of extracellular vesicles (EVs) in the mouse serums 35

Table 2.4 Properties of serum sEVs and expression of microRNAs 35

Table 3.1 Primary and secondary antibodies used in immunohistochemistry and western blot 53

Table 3.2 Primer sequences for qPCR.....54

Table 3.3 Measurements of extracellular vesicles (EVs) and exosomes in the mouse serums 56

LIST OF FIGURES

Figure 1.1 Histological analysis of the beagle placenta at late pregnancy 20

Figure 1.2 Distribution of the genes detected by RNA-Seq (MA plot).....21

Figure 1.3 RT-PCR analysis for the selected genes from RNA-Seq.....22

Figure 1.4 Western blot analysis on the canine serums at non-pregnancy, day 19, 41, and 51 of gestation (D19, D41, D51) 23

Figure 1.5 Exosomes characterization isolated from canine pregnant serum 24

Figure 1.6 Real-Time PCR analyses for relaxin (RLN) 2 25

Figure 2.1 Evaluation of immunostaining for CD9, CD63, and CD81 in the labyrinth region at Gd 18.5 using immunoreactive score (IRS) 41

Figure 2.2 Results of nanoparticle-tracking assays for the extracellular vesicles (EVs) isolated from mouse serums at non-pregnant (NP) and several gestational days (Gd) 42

Figure 2.3 Western blot and quantitative analyses of isolated EVs 43

Figure 2.4 Immunohistochemical staining on the mouse placental tissues at Gd 18.5 44

Figure 2.5 miRNAs in the serum EVs were detected by qPCR 45

Figure 3.1 Preeclampsia phenotype were observed in the L-NAME-induced PE mouse model 60

Figure 3.2 Histopathological examination of placenta 61

Figure 3.3 Characterization of extracellular vesicles (EVs) 62

Figure 3.4 Immunohistochemistry and western blot analyses of VEGF and iNOS in placenta tissues and serum-derived EVs from healthy pregnancy mouse and those with preeclampsia 63

Figure 3.5 miRNAs in the serum EVs were detected by qPCR 64

GENERAL INTRODUCTION

During pregnancy, several factors influence the physiology of both the mother and the developing fetus (Yang *et al.,* 2020). The mother and fetus share their antigens through the placenta and communicate through secreted factors such as extracellular vesicles (EVs), cytokines, and hormones ((Fader *et al.,* 2008; Czernek *et al.,* 2020). Communication between cells occurs through direct contact, soluble factors, intercellular nanotubes, and EVs (Jin *et al.,* 2018).

EVs can be categorized based on their biogenetic pathway, physical characteristics, and composition. There are three main subgroups of EVs, namely apoptotic bodies, microvesicles, and exosomes. This classification is based on the way they are formed, and released, and their size (Rajaratnam *et al.,* 2021). Exosomes are the smallest type of EVs, with an average diameter of 30–120 nm, that are secreted by various mammalian cells (Li *et al.,* 2019). Exosomes are produced through an endosome-dependent pathway and carry nucleic acids, proteins, lipids, cytokines, and metabolites (Bai *et al.,* 2021). They are released by fusing multivesicular bodies containing intraductal vesicles with plasma membranes. Exosomes are also associated with immune responses, viral pathogenesis, pregnancy, nervous system diseases, and cancer progression (Hoshino *et al.,* 2015; Asai *et al.,* 2015). Studies have demonstrated that exosomes play a crucial role in normal and complicated pregnancies (Guo *et al.,* 2023).

The concentration of exosomes in the bloodstream increases 50 times during pregnancy. These exosomes come from the placenta and contain proteins, lipids, and nucleic acids that can exert different biological effects on target cells and can represent the originating cell and its pathophysiological state (Mincheva-Nilsson, 2014; Salomon *et al.,* 2014). Exosomes can transfer RNA to target cells, where messenger RNA can be translated into protein and microRNAs can alter the gene expression of the recipient cell (Valadi *et al.,* 2007). Certain types of miRNAs are more common in exosomes, which come from specific cells (Mathivanan

et al., 2010). This process of sorting miRNA into exosomes is regulated, but not fully understood (Morales-Prieto, 2012). Exosomal miRNAs play a critical role in many physiological pregnancy processes. While the miRNA content in human placental-derived exosomes is known, the miRNA composition in the murine placenta is not yet fully understood (Landgraf *et al.,* 2007; Stefanski, 2019).

The placenta, a principal organ in pregnancy, is a temporary organ that plays a crucial role in controlling and regulating the communication between the mother and the developing child during pregnancy (Ji *et al.,* 2013). Placental cells of both maternal and embryonic origin, secrete not the simplest soluble endocrine mediators but additionally extracellular vesicles, along with exosomes (Czernek *et al.,* 2020). Exosomes play a critical role in pregnancy by modulating several processes including maternal immunologic response and metabolic adaptations. It identifies that the entire circulating exosomes in pregnancy increase across gestation (Nair and Salomon, 2018; Mitchell *et al.,* 2015; Sarker *et al.,* 2014). The placentas secrete large quantities of exosomes into the maternal circulation during normal pregnancy and more exosomes are released under pregnancy complications like preeclampsia, gestational diabetes, fetal growth restriction, and preterm birth that make it serve as useful biomarkers (Nair and Salomon, 2018).

Placenta-derived EVs (PEVs) have both local and systemic effects, coordinating various processes. PEVs are important mediators of the maternofetal interplay, influencing different fetal and maternal tissues and organs (Nakahara *et al.,* 2020). In humans, although syncytiotrophoblasts (STBs) are the main source of PEVs, other cell groups from the placenta such as cytotrophoblasts (CTBs), mesenchymal cells, and extravillous trophoblasts (EVTs) are also involved in their production (Kupper and Huppertz, 2022). The amount, biogenesis, content, and biological functions of PEVs differ significantly depending on the trimester of gestation and the physiological state of the feto-placental unit (Zhang *et al.,* 2020; Condrat *et al.,* 2021).

In contrast to human placental exosomes, the content of murine placental and pregnancy exosomes remains largely understudied. On the other hand, placental alkaline phosphatase (PLAP) is a molecular marker used to identify and classify placental extracellular vesicles (PEVs) in humans (Mincheva-Nilsson, 2021). However, for mice studies, syncytin is used as the marker for PEVs because PLAP is not expressed in mouse placenta (Skynner *et al.,* 1999). PEVs include exosomes, microvesicles, and apoptotic bodies, which can be detected in human maternal blood from 6 weeks of pregnancy and are known to steadily increase until they reach their highest concentration at term. In mice, PEVs can be detected at gestational day (Gd) 5, and the maximum number of exosomes was seen on day 18, just before delivery (Sheller-Miller, 2019b). Studies have shown that EVs are released in significant quantities from the placenta in humans and mice during pregnancy, and their concentration increases throughout gestational periods. However, there have been only a few studies on exosomes in dogs related to reproductive health, with no reports on exosomal concentration during pregnancy (Diomaiuto *et al.,* 2021). Research on horse exosomes concentration is restricted only in early pregnancy with no change in the overall amounts of exosomes in the serum of pregnant and non-pregnant mares (Klohonatz *et al.,* 2016). Therefore, a little investigation was done on mare serum exosomes just before parturition on week 46. The results showed no significant differences in exosome concentration (our unpublished data). Additionally, even though there is no difference in total amount, Klohonatz et al. (2016) revealed that the miRNA content of these exosome populations differs based on pregnancy status and may affect mRNA expression related to focal adhesion pathway in the endometrium with a potential role in maternal recognition of pregnancy, suggesting that maternal recognition of pregnancy is a complex process, therefore a multitude of miRNAs are actively involved and affect the gene that targeted by its miRNA.

OBJECTIVES OF THIS DISSERTATION

There are several pieces of evidence to suggest that exosomes have an important role in the maintenance of placental growth and fetal growth at the feto-maternal interface during normal pregnancy in mammals. However, the contents of exosomes remain to be fully determined. I address here about exosomal miRNA during a healthy and complicated pregnancy. The topics covered in this study include:

Chapter 1.

Humoral factors released from the placenta are known to influence the pregnancy progression, but the involvement of the canine placenta is often unidentified. This study was undertaken to investigate highly expressed genes in canine placentas and verify the possibility of a transition of these translated proteins into maternal blood, as well as to confirm the existence of cell-free RNAs packed in exosomes in the canine serums during normal pregnancy.

Chapter 2.

Exosomes are present in the blood of pregnant mice and are considered to be involved in pregnancy physiology. While it is thought that exosomes in pregnant periods are proposed to be derived from placentas, the cells that produce these exosomes are not well known in the mouse placenta. Thus, the appearance of exosomes in pregnant serum and their localization in placentas are investigated. This study is also examining how exosomal miRNA changes throughout pregnancy and its role in a healthy pregnancy for mice.

Chapter 3.

Dysregulation of angiogenetic factors interferes with the normal progression of pregnancy and is a cause of pre-eclampsia (PE). In this study, we investigated the dynamics of exosomes and variations of physiological factors and micro RNA (miRNA) contained in exosomes on the pathogenesis of preeclampsia.

CHAPTER 1

Specific expression and blood kinetics for relaxin 2, lipocalin 2, and tissue factor pathway inhibitor 2 at the canine placenta and pregnant bloods

1.1 Abstract

In general, humoral factors released from the placenta influence pregnancy progression, but the involvement of the canine placenta is often unidentified. We investigated specific genes in canine placentas and analyzed the blood dynamics of the translated proteins. Furthermore, RNAs are known to be released from placentas embedding in exosomes, a type of extracellular vesicles. Here, the presence of cell-free RNAs in pregnant serums was also confirmed. RNA specimens were purified from the normal healthy dog placentas and applied to RNA-Seq analysis. Expressions of frequent genes were confirmed by RT-PCR using placentas from other individuals and breeds. Relaxin (RLN) 2, lipocalin (LCN) 2, and tissue factor pathway inhibitor (TFPI) 2 were selected as highly expressed and placenta-specific genes. By western blot, the three factors were clearly detected in the pregnant serums. Quantitative analysis revealed that the amount of RLN2 increased significantly from non-pregnancy to day 41 of pregnancy. Regarding LCN2 and TFPI2, the protein serum levels elevated during pregnancy, but the statistical differences were not detected. Exosomes were found in all pregnant serums; however, the percentage was less than 6% in total extracellular vesicles. The cell-free RNA related to RLN2 was detected, but no elevation was confirmed during pregnancy. We found specific genes in the canine placenta and the transition of their translated protein into the blood. These factors may become useful tools for research on canine pregnancy and monitoring of reproductive management. Exosomes and cell-free RNA could not be found to be valid in canine reproduction.

1.2. Introduction

The placenta is a multifunctional organ that performs substance exchange between embryo and mother, establishes immune tolerance against fetal tissues, and directs the maternal endocrine conditions to pregnancy acceptance and maintenance. Maternal internal conditions

alter during gestation, especially in the cardiovascular, pulmonary, immune, and metabolic systems and they are suggested as pregnancy adaptive responses with placenta-derived factors (Nair and Salomon, 2018). Several factors relating to placentas have been reported, which are suggested to modulate the maternal physiological conditions to promote pregnancy maintenance, nutrition mobilization, delivery, and lactation (Mastorakos and Ilias, 2003; Velegrakis *et al.,* 2017). Among domestic animals, the canine placentas show a unique reproductive physiology, which has a low capacity for steroid synthesis (Hoffman *et al.,* 1994, Kowalewski *et al.,* 2020). The progesterone (P4) profiles in gestation are similar to the estrous cycles with non-pregnant. There is no remarkable elevation of estrogen (E2) before the parturition. Therefore, neither P4 nor E2 serves as useful markers for pregnancy monitoring in dogs (Concannon *et al.,* 1989; Hoffmann *et al.,* 1994). Consequently, the identification of novel markers is required for monitoring canine pregnant progression. At present, relaxin (RLN) is regarded as the only valuable marker for pregnant dogs. Originating from the placentas, canine RLN is detectable in the maternal blood around the third or fourth week of pregnancy (Nowak *et al.,* 2017; Steinetz *et al.,* 1987).

The onset times of pregnancy-specific changes have been estimated, including the formation of embryo sacs (about day 19), palpable uterine enlargements (day 21), finding fetal heartbeats (day 24), the elevation of blood prolactin (day 35), and radio-opaque fetal details (day 46) (Concannon *et al.,* 1989). The canine placentation process begins around day 14 when the yolk sac placenta is formed and continues to day 15 when the allantoic sac expands, and day 20 when the chorioallantoic membrane is formed. Completed the chorioallantoic placenta forms a barrier structure for fetuses against infectious microorganisms and toxic molecules as well as functions for nutrients and oxygen supply. Better insight into the expression of placenta-specific genes seems to reflect not only the process of placental formation but also the placental function that is needed for fetal health.

Exosomes are the smallest type of extracellular vesicles (EVs), 30–150 nm in diameter (Chernyshev *et al.,* 2015; van der Pol *et al.,* 2014), secreted by many types of cells (Colombo *et al.,* 2014; Tkach and Thery, 2016). The exosomes encapsulate a variety of biological cargo, such as nucleic acids, lipids, and proteins. These transportations by exosomes can influence target cell function and exert cell-to-cell communication (Zhang and Chop, 2016). In pregnant humans and mice, placenta-derived exosomes are found in maternal circulation across the placental barrier and reach maximum numbers at term (Jin and Menon, 2018; Mitchell *et al.,* 2015, Nair and Salomon, 2018; Salomon *et al,* 2013; Sarker *et al.,* 2014). The placenta-derived exosomes are suggested to participate in the normal processes of placental development and maternal immune tolerance (Stenqvist *et al.,* 2013). The cell-free nucleic acids transferred by exosomes have the possibility to enhance cell signaling processes in recipient cells not only in the range of normal physiology but also in pathological conditions (Heusermann *et al.,* 2016, Lakhal and Wood, 2011; Liu *et al.,* 2013; Vallhov *et al.,* 2011). However, the appearance and functions of exosomes relating to canine pregnancy remain unclear and need to be confirmed.

The specific goals of this study are to clarify highly expressed genes in normal canine placentas and to verify the possibility of a transition of these translation products into maternal blood. We validated the dynamics of the candidate factors in the gestational period and proposed usefulness for early pregnancy diagnosis and monitoring of a healthy pregnancy course. Finally, we confirmed the existence of exosomes in the canine pregnant blood and the possibility of transport vehicles for the placenta-derived candidate factors.

1.3. Materials and Methods

1.3.1. Animal samples

Canine placenta and uterine samples were collected from the veterinary hospitals with research cooperation after informed consent from the owners. Placenta samples of Beagle were

obtained by the operation of ovariohysterectomy. The gestational age was estimated to be 50 days old based on the crown-rump length of fetuses. From pregnant Maltese and Toy Poodle, and another pregnant individual of Beagle, placentas were collected by the cesarean operation (at full term). Non-pregnant uteri were collected by the sterilization operations from the Shiba and Beagle.

Serum samples were obtained from three Beagles under the rearing management in KBT Oriental (Saga, Japan). Blood was collected from the cutaneous vein of the forelimb and centrifuged. Serum was collected from the same individuals during the non-pregnant period and at days 19, 41, and 51 of pregnancy.

ICR mice were purchased from Japan SLC (Hamamatsu, Japan). At 8 weeks of age, they were administered anesthetics by isoflurane and euthanized by cervical dislocation. One pair of male and female cohabited, and gestation was defined as day 0.5 of pregnancy by checking the vaginal plug on the next morning. The large intestine, heart, kidney, and placenta (day 14 of pregnancy) were collected for the control tissues of western blot. Experiments using mice passed preliminary reviews by the Ethical Committee on Animal Experimentation at Yamaguchi University (Approval numbers: 479).

1.3.2. Histological analysis

A histological study was conducted on the Beagle placentas (estimated day 50 of pregnancy). The formalin-fixed tissue sample was dehydrated, permeated, paraffin-penetrated, and embedded in paraffin blocks. Sections of 5 μm thickness were prepared using a sliding microtome, and H-E staining was performed by a conventional method.

1.3.3. RNA isolation and RNA-Seq analyses

Two Beagle placentas estimated day 50 of pregnancy were used for the RNA-Seq study. Tissues were trimmed to 10 mm square specimens in RNA later solution (Thermo Fisher Scientific, Waltham, MA, USA) to include all tissue layers of the canine placenta (Fig. 1A).

Specimens were homogenized with ISOGEN II (Nippon Gene, Tokyo, Japan) using Multi Beads Shocker (Yasui Instrument, Osaka, Japan). Total RNA was isolated following the protocols in the ISOGEN II manual. RNA sequencing was performed at Yamaguchi University Center for Gene Research using Illumina NextSeq (Illumina, San Diego, CA, USA). The number of RNA reads and the correlation of gene expression frequency between the two placentas was confirmed using the RaNA-seq platform (https:// ranaseq.eu/index.php). The highly expressed genes commonly in two placentas were searched. These RNA-Seq data were available in DDBJ Sequence Read Archive (DRA) by accession No. SAMD00508674.

1.3.4. RT-PCR analysis

Highly expressed genes obtained from RNA-Seq were confirmed individually by RT-PCR analysis. This analysis was performed on the placentas collected from different breeds of dogs (Maltese, Toy Poodle, and Beagle at full term) and on the non-pregnant uteri from the Shiba and Beagle. Complementary DNA (cDNA) was synthesized from total RNA by reverse-transcription by ReverTra Ace qPCR kit (TOYOBO, Osaka, Japan). The PCR reaction was performed by Go-Taq (Promega, Madison, WI, USA) with T100 Thermal Cycler (Bio-Rad, Hercules, CA, USA) using each primer set (Supplementary Table 1). Canine mRNA sequences were referred from a database in Ensembl (Cambridge, UK) and primer sequences were designed using the pick primer function on the GenBank homepage (Bethesda, MD, USA). Glyceraldehyde-3-phosphate dehydrogenase (GAPDH) primers were used for an internal control reaction. Sizes of PCR products were confirmed by agarose gel electrophoresis.

1.3.5. Western blot analysis

The protein concentrations of serum samples were measured by NanoDrop 2000 (Thermo Fisher Scientific) and diluted to 1.5–2 mg/mL with CHAPS buffer (10 mM CHAPS, 0.15 M NaCl, 0.01 M sodium phosphate, 2 mM EDTA, pH 7.2). The proteolytic enzyme inhibitors (10 mg/mL phenylmethylsulfonyl fluoride, 100 mM sodium vanadate, 10 mg/mL

aprotinin) were added to the CHAPS buffer. Following a mix with the sample buffer [2-mercaptoethanol 50 μL, 2 × Laemmli Sample Buffer (Bio-Rad) 950 μL], specimens were conducted with heat denaturation at 90°C for 10 min. Protein samples were electrophoresed using 4–12% Invitrogen Bolt Bis-Tris Plus gel (Thermo Fisher Scientific). Transblotting to a polyvinylidene difluoride membrane was performed using a transfer device (ATTO Blotting System, Tokyo, Japan). Immunoblotting was conducted as follows, blocking with 5% bovine serum albumin for 30 min, the primary antibody at 4°C overnight, and the secondary antibody at room temperature for 1 hr. The information on the primary antibody is shown in Supplementary Table 2. The chemiluminescence reaction was detected with ECL Pro western blotting Detection Reagent (PerkinElmer, Waltham, MA, USA) and Amersham ImageQuant 800 (Cytiva, Tokyo, Japan).

Mouse tissues for positive controls were trimmed into RIPA buffer (1% nonidet P-40, 1% sodium deoxycholate, 0.1% SDS, 0.15 M NaCl, and 2 mM EDTA in 0.01 M sodium phosphate buffer, pH 7.2) and proteolytic enzyme inhibitor mentioned above. Tissues were crushed with a homogenizer (T10 Basic, IKA, Vernon Hills, IL, USA) and allowed to stand on ice for 30 min for protein extraction. The supernatant was obtained after centrifugation at 4°C and 5,000 × g for 20 min.

1.3.6. *Isolation of extracellular vesicles (EVs)*

Serum samples were centrifuged by 2,000 × g for 30 min at 4°C to remove cell debris. Supernatants were transferred to new microcentrifuge tubes and mixed with Invitrogen Total Exosome Isolation reagent (Thermo Fisher Scientific). After incubation at 2–8°C for 30 min, centrifugation was conducted by 10,000 × g for 10 min at room temperature. The pellet was collected and re-suspended with cold phosphate buffer saline (PBS) filtered with the 0.22 μm pore-size membrane. Purified EVs were measured for the size and concentration using a nanoparticle imaging analyzer (Videodrop, Myriade, France).

1.3.7. *Observation of EVs using transmission electron microscopy (TEM)*

Purified EV samples were fixed with 4% paraformaldehyde for 10 min at room temperature. Ten μL of suspended samples were loaded on the grid with a 20 nm carbon membrane (EM Japan, Tokyo, Japan), incubated for 20 min, and fixed again with 1% glutaraldehyde for 5 min. After rinsing with a drop of 10 μL filtrated PBS, grids were stained with 1% uranyl acetate for 5 min. After drying overnight at room temperature, the grid was then placed in a specimen holder of H-7100 electron microscope (Hitachi, Tokyo Japan). The images were captured at × 15,000–30,000 magnification.

1.3.8. *Cell-free RNA purification and real-time PCR analysis*

Cell-free RNA was purified from canine serum specimens using the kit of small RNA and DNA from plasma (Macherey-Nagel, Düren, Germany). RNA yields were measured using NanoDrop 2000 and cDNA synthesis was conducted as explained above. Real-time PCR was performed with the KAPA SYBR FAST kit (Nippon Genetics, Tokyo, Japan) and CFX96 Touch Real-Time PCR Detection System (Bio-Rad). Primer sequences were the same as the ones for RT-PCR analyses (Supplementary Table 1). Specificities for each reaction were confirmed by the amplification plots and the melting curves for the double-stranded PCR products.

1.3.9. *Statistical analysis*

Images of western blotting were quantitatively analyzed using Image J software (NIH, Bethesda, MD, USA), and the data were corrected by the protein concentration of each sample. All data were presented as means ± standard deviation. On the two experimental groups, a two-sample t-test was conducted when F-test indicated the equal variance among two groups, or the Welch t-test was conducted when unequal variance was confirmed. Significant differences were considered when P-value was less than 0.05. In addition, Bonferroni correction was applied when the statistical analysis corresponded to the multiple comparisons.

1.4. Results

1.4.1. Histological observation

Matured canine placenta exhibited layered structures (Fig. 1.1A), which can be divided into maternal tissues (a–c) and a mixture of fetomaternal derivation (d, e). The spongy layer (c) was composed of significantly enlarged uterine gland ducts. The ductal epithelial cells showed abundant numbers of extracellular vesicles (Fig. 1.1B).

1.4.2. Gene expression of canine placentas by RNA-Seq and RT-PCR

Statistical analysis from RNA-Seq indicated frequency distributions of expressed genes (Fig. 1.2) and a positive correlation between the two dog placentas. The genes commonly detected in two placentas were arranged in order of mean values of frequency (Table 1.1). Unidentified genes were excluded for further analysis. Local expressions of listed genes were confirmed by RT-PCR (Fig. 1.3). The nine factors (TMSB10, S100P, WFDC2, GM2A, RBP4, HSBP1, LY6E, PFN1, and APOE) were detected in the placenta as well as the non-pregnant uterus. NPPC did not show clear bands in the placentas of all dog breeds. Expressions of RLN2, lipocalin (LCN) 2, and tissue factor pathway inhibitor (TFPI) 2 were detected to be specific in the placentas and not in the uteri. LCN2 was undetectable in the Beagle placentas, which were collected from the other individuals used in RNA-Seq. RLN2 and TFPI2 were commonly detected in the placentas of all three-canine species. Thus, the following experiments were conducted focusing on RLN2, LCN2, and TFPI2.

1.4.3. Western blotting on canine pregnant serums

RLN2, TFPI2, and LCN2 were investigated for their presence as soluble proteins in the serums and the variations during pregnancy periods (Fig. 1.4A). Serum protein levels of RLN2 were found to be significantly increased at D41 and D51 compared to non-pregnant (Fig. 1.4B). Serum TFPI2 showed an increase at D19 and D41, but no significant difference from the non-pregnant period. TFPI2 level decreased significantly at D51 (Fig. 1.4C). LCN2 also showed

similar blood dynamic from non-pregnancy to pregnancy stages as TFPI2 (Fig. 1.4D).

Table 1.1. Highly expressed genes in the canine placentas at late pregnancy

Frequency ranking	Gene name	Gene ID	Frequency of dog placenta 1	Frequency of dog placenta 2	Mean values of frequency	Note
1	*TMSB10*	ENSCAFG00000007875	2,30E+05	31395,3	1,30E+05	
2	*ENSCAFG00000012272*	ENSCAFG00000012272	2436,41	1,20E+05	6,20E+04	Unidentified gene
3	*ENSCAFT00000046268.1*	ENSCAFG00000030508	7126,99	12777,78	9952,38	Unidentified gene
4	*ENSCAFG00000022729*	ENSCAFG00000022729	7214,28	11480,45	9347,36	Unidentified gene
5	*RLN2*	ENSCAFG00000002115	18161,35	14,37	9087,86	
6	*ENSCAFG00000022726*	ENSCAFG00000022726	7202,06	10585,90	8893,98	Unidentified gene
7	*ENSCAFG00000022730*	ENSCAFG00000022730	7343,10	10271,15	8807,12	Unidentified gene
8	*ENSCAFG00000022723*	ENSCAFG00000022723	7412,45	9879,35	8645,90	Unidentified gene
9	*APOE*	ENSCAFG00000004617	9971,54	6762,68	8367,11	
10	*NPPC*	ENSCAFG00000011135	13627,95	647,42	7137,69	
11	*TFPI2*	ENSCAFG00000002040	12536,55	927,73	6732,14	
12	*WFDC2*	ENSCAFG00000009696	245,82	13179,90	6712,86	
13	*RBP4*	ENSCAFG00000007893	379,35	12976,80	6678,08	
14	*ENSCAFT00000009976.4*	ENSCAFG00000030286	11463,73	1397,55	6430,64	Unidentified gene
15	*ENSCAFG00000032122*	ENSCAFG00000032122	5923,25	5801,78	5862,52	Unidentified gene
16	*GM2A*	ENSCAFG00000057252	11495,78	166,33	5831,05	
17	*LCN2*	ENSCAFG00000020088	11121,38	23,05	5572,21	
18	*ENSCAFG00000029904*	ENSCAFG00000029904	9434,57	1317,55	5376,06	Unidentified gene
19	*PFN1*	ENSCAFG00000015827	4261,18	6417,86	5339,52	
20	*ENSCAFG00000030265*	ENSCAFG00000030265	3264,36	7159,62	5211,99	Unidentified gene
21	*LY6E*	ENSCAFG00000001289	322,92	8042,54	4182,73	
22	*HSBP1*	ENSCAFG00000019973	899,24	7165,64	4032,44	
23	*S100P*	ENSCAFG00000014333	6303,81	1559,30	3931,56	

APOE: Apolipoprotein E
GM2A: GM2 ganglioside activator
HSBP1: Heat shock factor binding protein 1
LCN2: Lipocalin 2
LY6E: Lymphocyte antigen 6 family member E
NPPC: Natriuretic peptide C
PFN1: Profilin 1
RBP4: Retinol binding protein 4
RLN2: Relaxin 2
S100P: S100 calcium binding protein P
TFPI2: Tissue factor pathway inhibitor 2
TSMB10: Thymosin beta 10
WFDC2: WAP four-disulfide core domain 2

1.4.4. Analysis of exosomes in canine pregnant serum

By TEM observation, single, even-sized, and ball-shaped EVs were confirmed from all serum samples, allowing appropriate size for the exosomes (Fig. 1.5A). However, the percentage of exosomes in total EVs was low (Fig. 1.5B). Average diameters in total EVs were 300–400 nm (Table 1.2), which was a considerably larger range than the standard size of exosomes. Concentrations of total EVs were higher at non-pregnant serums than during

pregnancy periods. The highest percentage of exosomes in total EVs showed 5.68% in the serum from day 19. At day 19 of pregnancy, concentration of exosomes was estimated to be 12.0×10^8 numbers/mL.

Table 1.2. Measurements of extracellular vesicles (EVs) and exosomes in the canine serums

	Non-pregnant	Day 19	Day 41	Day 51
Average diameter in total EVs (nm)	412 ± 19.0[a]	324 ± 28.2[a,b]	494 ± 36.5[b]	394 ± 34.1
Concentration of total EVs ($x10^9$/mL)	25.8 ± 2.61[c]	21.2 ± 2.64	17.6 ± 2.22[c]	21.2 ± 2.30
Rate of exosome-sized vesicles in total EVs (%)	1.20 ± 0.229	5.68 ± 3.00	1.27 ± 0.625	2.27 ± 0.875
Calculated concentration of exosomes in serum ($x10^8$/mL)	3,1	12,0	2,2	4,8

[a-c] Significant differences were found between the same alphabet. [b] $P<0.01$; [a,c] $P<0.05$. Bonferroni correction for multiple comparisons was applied.

1.4.5. Analyses of cell-free RNA in the serum

Real-time PCR analyses were conducted on the cell-free RNA purified from canine serum at non-pregnant and day 19 of pregnancy. Amplification of β-actin was not stable in all samples, and even in those that can be amplified, the Cq values were very large, ranging from 34–37 (data not shown). On the other hand, amplification of RLN2 was observed in all samples of both groups (Fig. 1.6A). However, the Cq values were 27.5 ± 0.35 (NP) and 27.9 ± 0.14 (D19) respectively (Fig. 1.6B), so no significant difference was detected. All peaks of the melting curve fell within the range of 74.5-75.0°C, suggesting that the PCR products from all samples were of similar sequences. Analysis of LCN2 and TFPI2 showed the same results with β-actin: the amplification reactions were not stable and the Cq values were very large (data not shown).

1.5. Discussion

From this study, we could propose here that RLN2, LCN2, and TFPI2 are specific expressing factors in the matured canine placentas commonly in dog breeds. These factors were readily detected in the pregnant serums by western blot, especially RLN2, which showed a significant increase in protein levels at days 41 and 51 of pregnancy compared to non-pregnant serums.

Relaxin has already focused on its usefulness in dogs as a blood marker for pregnancy diagnosis. Relaxin begins to increase around 25–30 days after LH surge, and peaks around 35 days gestation (Nowak *et al.,* 2017). These descriptions are consistent with our results. Relaxin assists fetal delivery by relaxing the pubic symphysis during labor. Furthermore, relaxin is involved in angiogenesis at the human endometrium, by promoting the expression of vascular endothelial growth factor (Unemori *et al.,* 1999). There are 1–3 subtypes in the relaxin family, and RLN2 is known to be highly expressed in human placentas (Rocha *et al.,* 2013). A continuous increase of RLN2 until late pregnancy periods may be a good indicator for the expansion of angiogenesis in the canine placentas and may reflect the increased demand for blood nutrients by the canine fetuses.

LCN2 is a secretory glycoprotein and has an iron-chelating ability, involving iron homeostasis, immune responses, and epithelial cell differentiation (Santiago-Sanchez *et al.,* 2020). LCN2 is also named neutrophil gelatinase-associated lipocalin (NGAL) and can be applied as a biomarker for acute kidney injury (Shang and Wang, 2017). Plasma levels of LCN2 become higher in pregnant women than in non-pregnant women (Cesur, *et al.,* 2012). Detection of LCN2 in human placentas has been reported in the cytotrophoblasts, the extravillous trophoblasts (EVTs), and the decidua at early periods (Kobara *et al.,* 2013; Tadesse *et al.,* 2011). In humans and rodents, vascular remodeling in the pregnant uterus is considered an essential process in normal placentation, and invasion of EVTs to the uterine spiral arteries is essential

for vascular remodeling (Pollheimer and Knofler, 2012). The invasive EVTs require matrix metalloproteinase (MMP)-2 and MMP-9 for the digestion and remodeling of the extracellular matrix (Burton *et al.,* 2009; Cohen *et al.,* 2006; Kobara *et al.,* 2013). LCN2 can bind to MMP-9 and prevent MMP-9 degradation (Brosens *et al.,* 1972). LCN2 expression and MMP-9 activation are enhanced under the hypoxic state, which is the normal biological environment in the human placenta. LCN2 may be useful for the investigation of the specific placental environment in relation to normal oxygen levels.

The canine placentas do not have EVT, but the trophoblasts also have invasive capacity. The factors responsible for the invasive activity are not well understood. The reason why LCN2 was not detected in the beagle placentas in RT-PCR may depend on the gestation date of the samples. The beagle placentas used for RNA-Seq were approximately day 50 of pregnancy, and the ones in RT-PCR confirmation were approximately day 60, just prior to parturition. LCN2 may not be required to maintain placental structures and functions in this stage. LCN2 could be a useful factor in the study of canine trophoblast invasiveness and may be an indicator of the activity of placentas during gestation.

TFPI2, also as a matrix-associated serine protease inhibitor, has been found in human placentas, especially in the vascular endothelial cells and the microvilli of placental syncytiotrophoblasts (Ali *et al.,* 2018; Miyagi *et al.,* 1994; Udagawa *et al.,* 2002). The function of TFPI2 is proposed to promote trophoblast invasion by relating to MMP-2 and MMP-9 expressions (Zheng *et al.,* 2020). On the other hand, TFPI2 can suppress the tissue factor and inhibit blood coagulation (Udagawa *et al.,* 2002). Elevation of TFPI2 is considered a compensatory reactivity that reflects beneficial adaptations to maintain blood coagulation homeostasis (Geddings and Mackman, 2013; Hoover-Plow, 2010). It is suggested that over-methylation of the TFPI2 promoter region determines the malignancy and prognosis for diffuse large B-cell lymphoma in dogs (Ferraresso *et al.,* 2014). Dog placentas contain the regions of

marginal hematoma, which destroys maternal erythrocytes and supplies iron nutrients to the fetus. Inhibition of maternal blood coagulation may be an essential element for placental nutritional function. Furthermore, TFPI2 may have a role in the regulation of cell proliferation and tissue formation in canine placentation.

Although we conclude that the other detected genes were not specific to dog placentas, there are relevant reports from the animal placentas of other species. RBP4 is involved in human trophoblast cell proliferation and infiltration (Li *et al.,* 2018). TMSB10 is suggested to be associated with ovine and porcine conceptus elongation (Smith *et al.,* 2001). In the previous study, many genes have been detected in human placentas, but the proportion of genes that functions related to pregnancy physiology and placental biology was estimated to be about 12% (Hou *et al.,* 2009). Appropriate comparison with expressed genes in normal placentas from those of abnormal pregnancy or gynecological diseases will find more important genes or factors.

In mice, exosomes can migrate the fetomaternal boundary in the placenta bidirectionally (Sheller-Miller *et al.,* 2019a). The exosomes made in the maternal tissues can influence fetal development or the progression of the pregnancy. The ones made in the fetal tissues can transfer into maternal blood and become a monitoring tool for the physiological status of fetuses (Sheller-Miller *et al.,* 2019b). In our study, exosomes in pregnant mouse serum showed up to 82.9% in the total EVs and the densities were in the range of 1.0–9.0 × 10^{11} numbers/mL (manuscript in preparation). In this study, however, the proportion of canine serum exosomes was only 5.68% of total EVs at most, and the calculated density was less three digits than those of mice. Histological study found a numerous number of secretory vesicles at the spongy layer, but they were large in size and may be better classified as microvesicles or cell debris rather than exosomes. Alternatively, the canine placenta has an endotheliochorial type and thick-layered fetomaternal boundary compared with the hemochorial type in mouse and human, so the exosomes produced in fetal tissue may be difficult to be transmitted to maternal blood. On the

other hand, canine exosomes showed a slight increase on day 19. Highly sensitive detection techniques may provide insight into the appearance and significance of canine exosomes during gestation.

The specific detection of RLN2 in cell-free RNA indicated that this mRNA was present in serum above a certain amount. However, the detective sensitivity of RLN2 on day 19 did not correlate with changes in canine exosome concentrations during gestation, suggesting that RLN2 does not increase significantly. On the other hand, the successful detection of RLN2 indicated the possibility of specific marker genes for cell-free RNA. Although their role may be smaller than in mice and humans, exosome-encompassing factors may be present and reflect fetal development and placental formation in the canine pregnant serum.

Here, using available RNA-Seq datasets derived from the dog placentas, we investigated valuable factors that are abundant in the pregnant serum and highly variable during gestation periods. We detected three genes specifically expressed in the canine placenta: RLN2, LCN2, and TFPI2. Increased protein levels of these factors in serum were thought to be involved in the regulations of angiogenesis, trophoblast invasion, and blood coagulation in the canine placenta in the normal course of pregnancy. The presence of exosomes and cell-free RNA, as well as serum proteins, were confirmed in canine pregnancy serums. Placenta-derived genes can be an effective tool for monitoring conditions for maternal endocrine, fetal growth, and successful pregnancy progression. Our results may contribute to the elucidation of canine pregnancy physiology and applications of clinical reproduction.

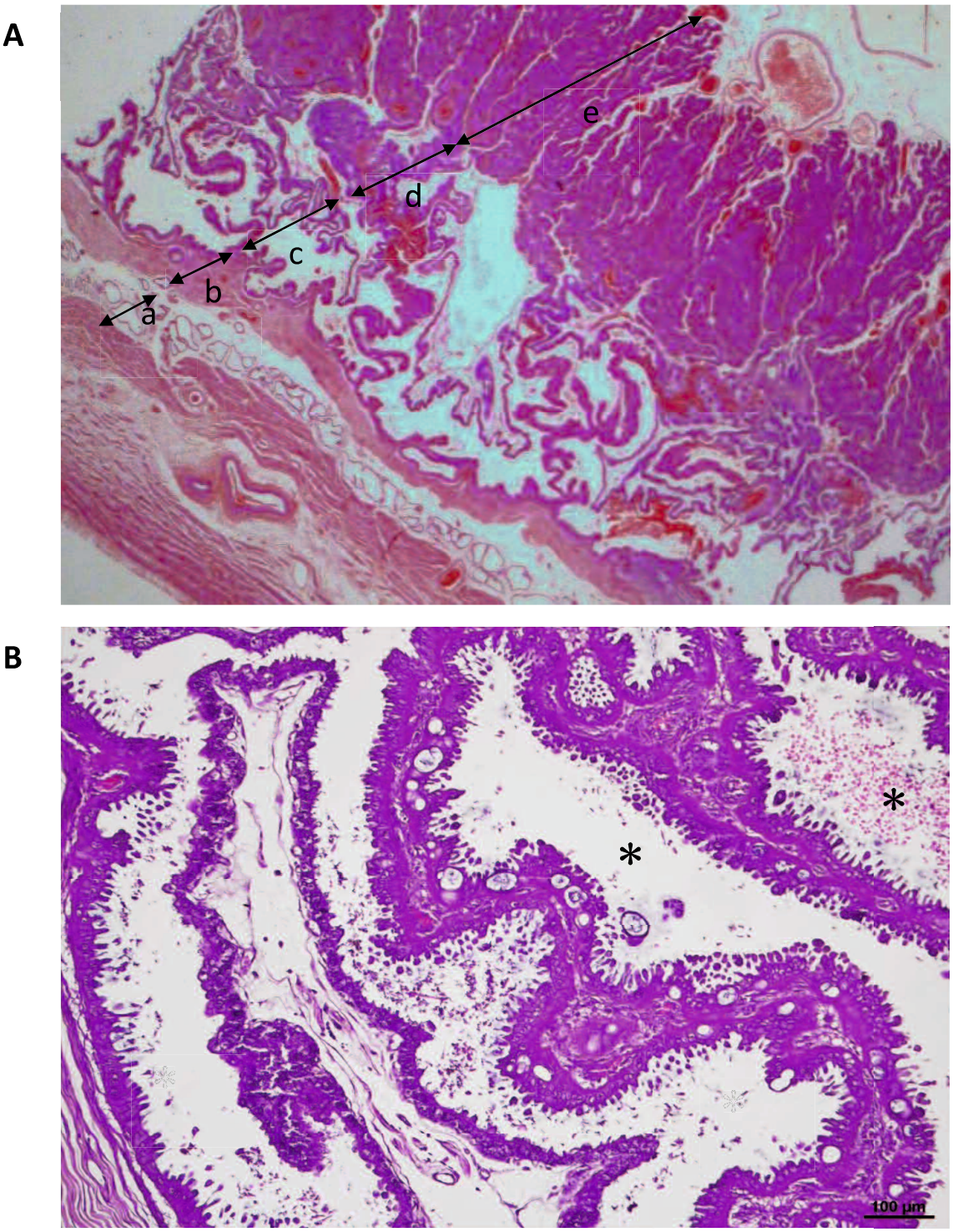

Figure 1.1. Histological analysis of the Beagle placenta at late pregnancy. (A) Observation at low magnification exhibited layered structures including the deep glandular (a), supra-glandular (b), spongy (c), junctional (d), and placental labyrinth layers (e). (B) Higher magnification of the spongy layer in another section. Dilatation on the uterine gland lumens was notable (*) and the epithelial cells of the uterine ducts develop many extracellular vesicles at the apical face.

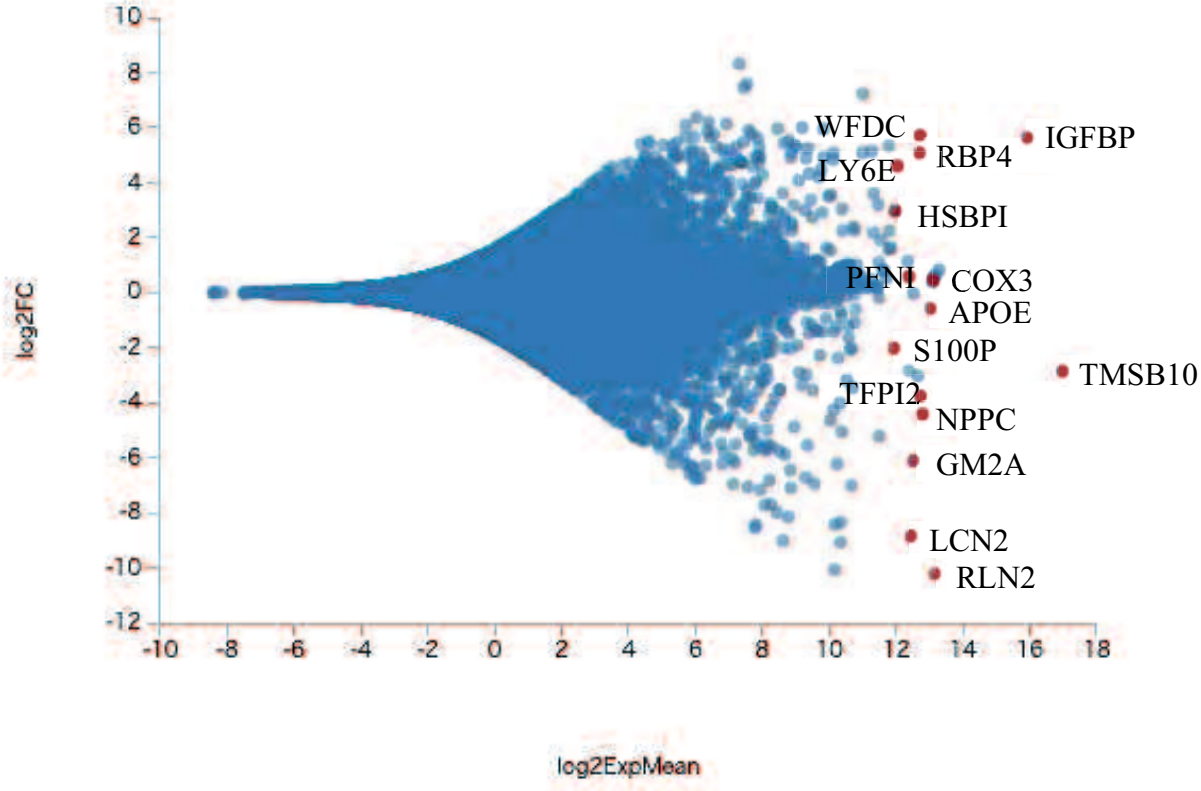

Figure 1.2. Distribution of the genes detected by RNA-Seq (MA plot), showing normalized mean values for expression frequency in the x-axis and expression ratios between the two Beagle placentas in the y-axis. A zero point on the y-axis indicates the distribution of genes that are equally expressed in both placentas. Highly expressed genes were selected as red plots and gene names were labeled.

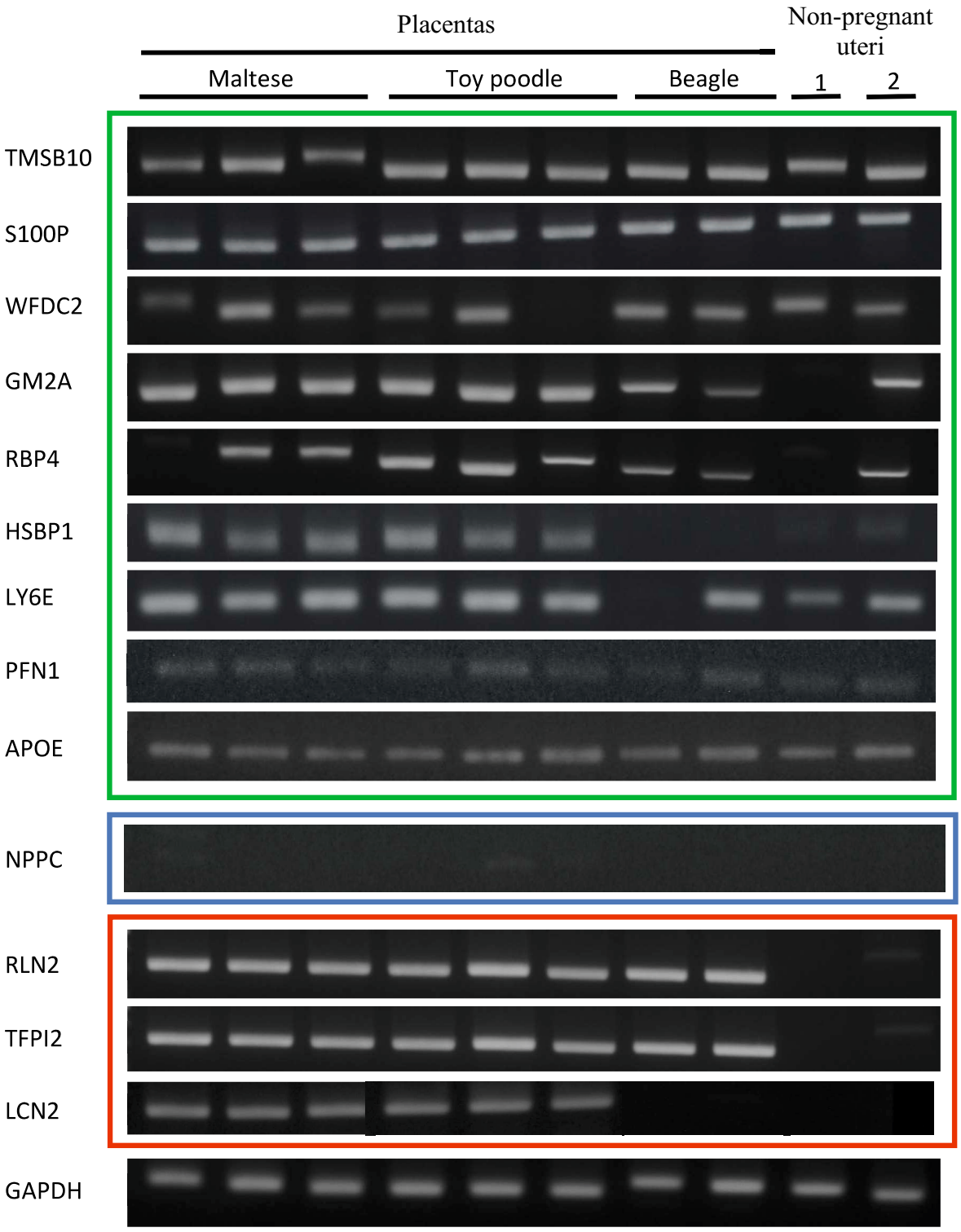

Figure 1.3. RT-PCR analysis for the selected genes from RNA-Seq. Local expression was confirmed on the independent placentas collected from three dog breeds and non-pregnant uteri from two breeds (lane 1: Beagle, lane 2: Shiba). The green box indicates the group with no confirmed gene expression in the placenta only. The blue box shows the gene group that any expression was confirmed in both tissues. Relaxin (RLN) 2, lipocalin (LCN) 2, and tissue factor pathway inhibitor (TFPI) 2 (red box) were confirmed to be expressed only in the placental tissues. Glyceraldehyde-3-phosphate dehydrogenase (GAPDH) expression shows internal control.

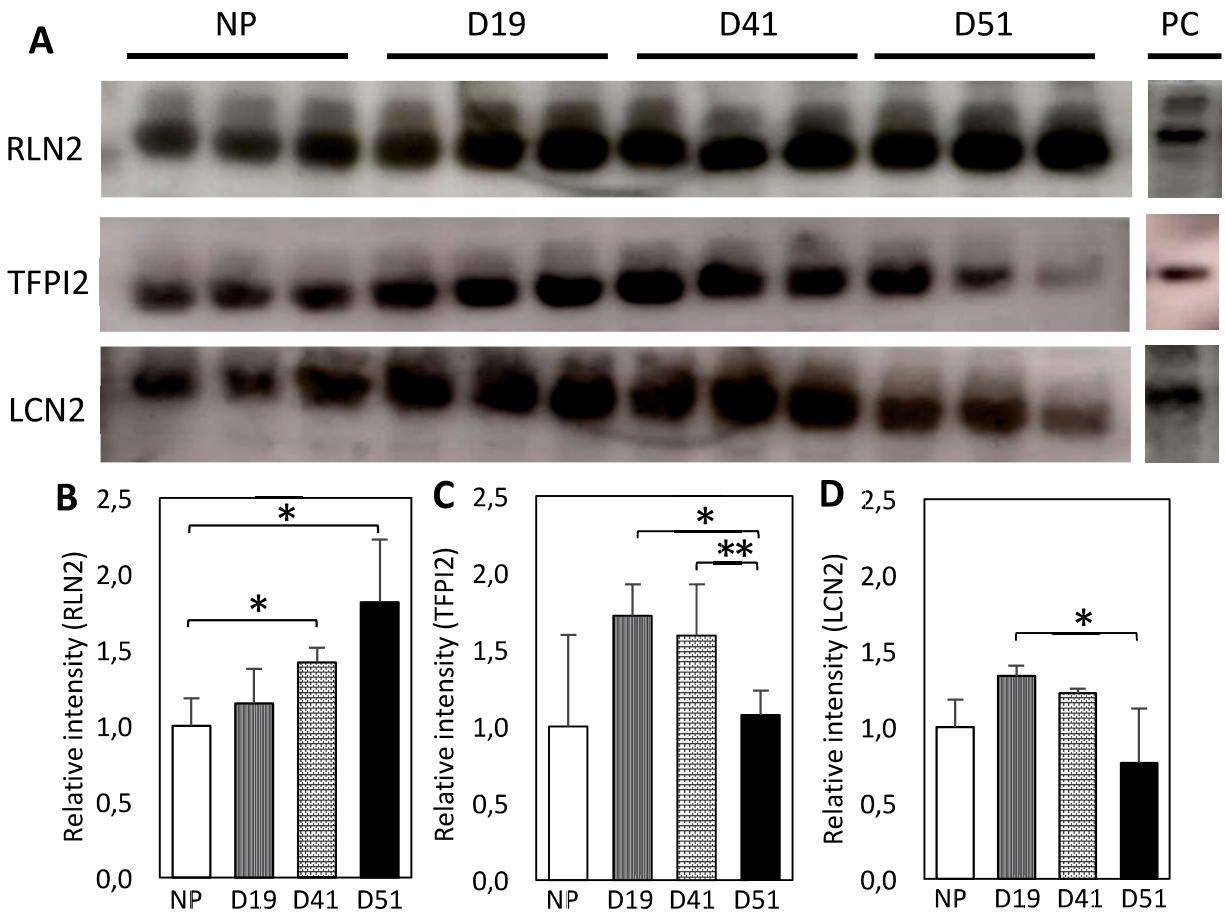

Figure 1.4. (A) Western blot analysis on the canine serums at non-pregnancy (NP), day 19, 41, and 51 of gestation (D19, D41, D51). Positive control (PC): mouse large intestine (for RLN2, LCN2) and mouse placenta tissue (for TFPI2). RLN: relaxin, LCN: lipocalin, TFPI: tissue factor pathway inhibitor. Molecular weight: 20.5 (RLN2), 26.2 (TFPI2), and 22.9 kDa (LCN2). (B–D) Quantitative analysis for the band densities on RLN2 (B), TFPI2 (C), and LCN2 (D). Measured values were normalized by the protein concentration of each sample. *P<0.05, **P<0.01 (Bonferroni correction for multiple comparisons was applied).

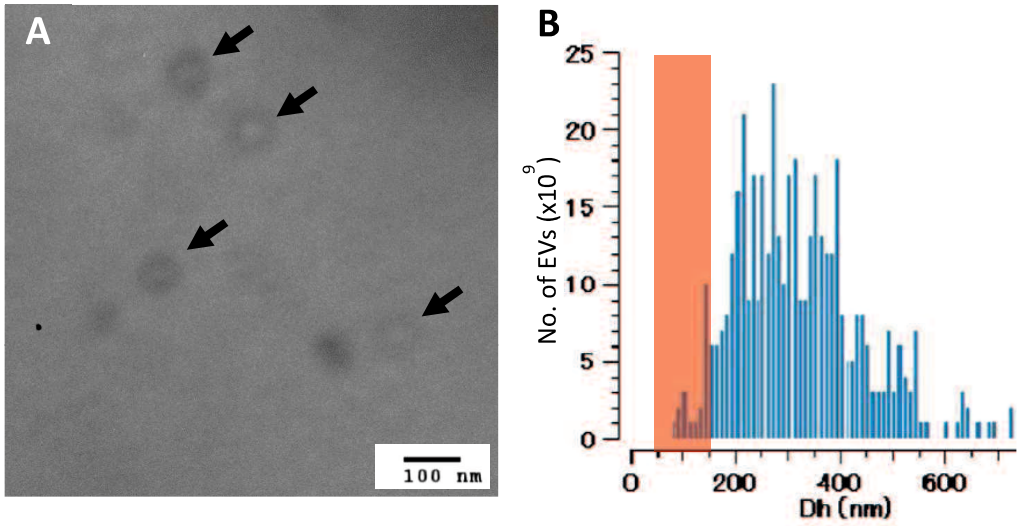

Figure 1.5. Exosomes characterization isolated from canine pregnant serum. (A) A photo by transmission electron microscope (TEM) for extracellular vesicles (EVs) in the serum at day 19 of gestation. Arrows indicate appropriately sized figures for exosomes. (B) An example of assays, showing a histogram of the numbers and sizes for the EVs on day 19 of pregnancy. The red area indicates a range for exosome size (30–150 nm in diameter).

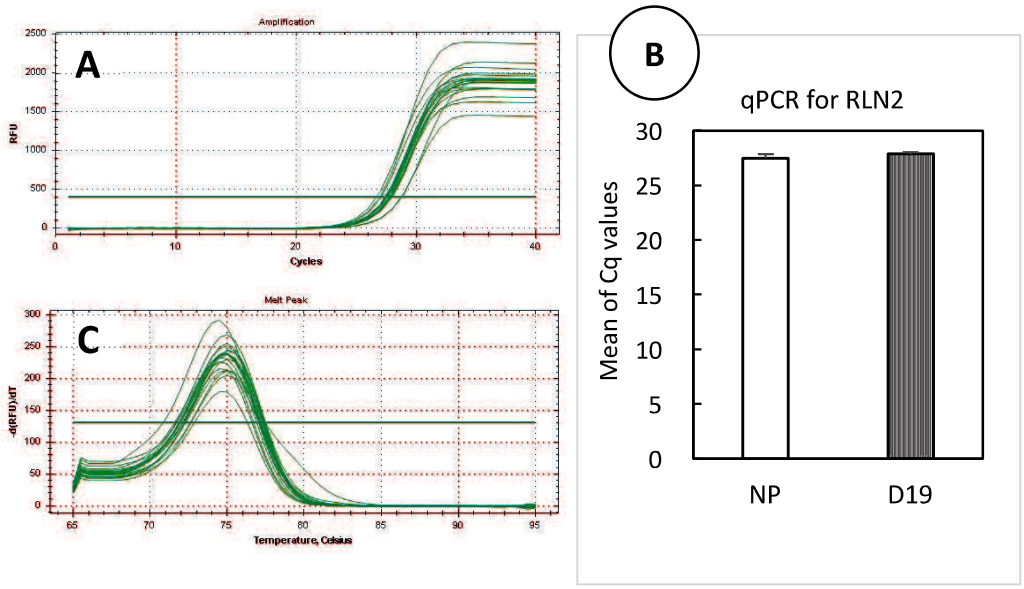

Figure 1.6. Real-Time PCR analyses for relaxin (RLN) 2. (A) Amplification plots of real-time PCR analyses for relaxin (RLN) 2. All samples of cell-free RNA in the canine serums at non-pregnant and day 19 of pregnancy showed a typical sigmoid curve shown by gene amplification. (B) There was no difference in the mean of Cq values in the samples between non-pregnant (NP) and day 19 of pregnancy (D19). (C) The melting temperature of the PCR product double-strand DNA showed 74.5–75.0°C for all samples.

CHAPTER 2

Appearance of exosomes in the mouse pregnant serum and the localization in placentas

2.1. Abstract

Exosomes are present in the blood of pregnant mice and are considered to be involved in pregnancy physiology. Although exosomes in pregnant periods are proposed to be derived from placentas, exosome-producing cells are not well known in mouse placentas. We studied the dynamics and localization of exosomes in pregnant serum and placentas, and examined gestational variation of microRNA (miRNA). Serums and placentas were collected from non-pregnant (NP) and pregnant mice throughout the entire gestational day (Gd). EVs were purified from serums and total RNA was isolated from EVs. Nanoparticle-tracking assay (NTA) revealed that the rates of exosomes in EVs are 53% at NP, and increased to 80.1% at Gd 14.5 and 97.5% at Gd 18.5. Western blotting on EVs showed positive reactivity to the tetraspanin markers and clarified that the results using anti-CD63 antibody were most consistent with the exosomes appearance detected by NTA. Serum exosomes also showed a positive reaction to the syncytiotrophoblast marker, syncytin-1. Immunohistostaining using anti-CD63 antibody showed positive reactions in mouse placentas at the syncytiotrophoblasts and endothelial cells of the fetal capillaries. Quantitative PCR revealed that significantly higher amounts of miRNAs were included in the exosomes of Gd 18.5. Our results suggested that exosomes are produced in the mouse placenta and transferred to maternal or fetal bloodstreams. exosomes are expected to have a miRNA-mediated physiological effect and become useful biomarkers reflecting the pregnancy status.

2.2. Introduction

In the placenta, not only the dams supply nutritional substances to the fetuses, but also the metabolites released from the fetuses transfer to maternal blood and fetal metabolites also correspond to the production of hormones or regulators that regulate normal pregnancy. Regarding the transportation of substances at the fetomaternal interface, roles of extracellular

vesicles (EVs), have been focused recently. Exosomes are a type of EVs, which are 30-150 nm in diameter and deliver nucleic acids, proteins, lipids, cytokines, and metabolites (Hessvik and Llorente, 2018; Raposo and Stoorvogel, 2013; Yanez-Mo *et al.,* 2015; Zaborowski *et al.,* 2015). Physiological properties of exosomes are characterized by stability and abundance in the bodily fluids, high fusibility with the cell membrane, and crucial roles relating to intracellular signaling (Bai *et al.,* 2021; Bang and Thum, 2012; Czernek and Düchler, 2020; Jin and Menon, 2018; Nair and Salomon, 2018). Several studies have shown that circulating exosomes in mice increase throughout gestation periods and reach the maximum before parturition (Nguyen *et al.,* 2019; Sheller-Miller *et al.,* 2019b. In humans, exosomes are detectable in the local tissues of the placenta, umbilical cord, amnion, and endometrium (Ghafourian *et al.*, 2022). These exosomes are thought to contribute to the establishment of pregnancy by embryo attachment, cell proliferation of extraembryonic cells, angiogenesis in placentas, and immune tolerance against maternal immune cells. The exosomes secreted from amnion at the late pregnancy periods can transmit inflammatory substances, and have an effect on the myometrium and cervix to induce the onset of parturition (Menon *et al.,* 2017). Mouse fetuses can produce exosomes containing different contents from those of dams (Sheller-Miller *et al.,* 2019a). The fetal exosomes accumulated in mouse placentas and parts of them were transferred to the maternal circulation (Stefanski et al., 2019). In human placentas, exosomes were produced locally at the extravillous trophoblasts, syncytiotrophoblasts (STs) (Mitchell *et al.,* 2015), cytotrophoblasts (Jin and Menon, 2018), and placental mesenchymal stem cells (Salomon *et al.,* 2013). Mouse placentas do not have the same type of cell equivalent to extravillous trophoblasts. The placental barrier in mice is formed by three layers of trophoblasts, called hemotrichorial (Steven, 1975). Human placentas have the hemomonochorial type and it differs from mouse placentas at the fine structure and cellular composition. Regarding exosome production and distribution, there is little clear evidence that indicates similarities and differences between human and mouse placentas.

CD9, CD63, CD81, and CD82 are classified into four transmembrane proteins and called tetraspanins. They are enriched on exosomes and EVs, and used as identification markers. Tetraspanins are required in the molecular processes of exosomes at the intermediate vesicle formation and the intraluminal release (van Niel *et al.,* 2018; Tognoli *et al.,* 2023). Furthermore, tetraspanins are involved in the cellular process for exosome uptake collaborating with adherent molecules (van Niel *et al.,* 2018). Several cancer cell lines release EVs possessing CD9 and CD81 and are frequently detected (Yoshioka *et al.,* 2013). The malignant cancer cells produce high amounts of CD63-positive EVs, whereas low in the non-cancer cell lines. CD9 and CD81 were detected as the top 200 most frequently identified as EV proteins of the eukaryotic cell lines (Kim *et al.,* 2013). However, less studies have explored the tetraspanin markers in pregnant serum and mouse placentas.

MicroRNAs (miRNAs) are typical contents of exosomes and have a role as bioactive mediators. The miRNAs are one of the small noncoding RNAs that can regulate gene expression by targeting messenger RNAs (Cheng *et al.,* 2014). It is suggested that miRNAs in maternal circulation influence the state of metabolism during pregnancy, and the variation of miRNAs is beneficial for finding pregnancy disorders such as preeclampsia and fetal intrauterine growth retardation (Loscalzo *et al.,* 2021; Lv *et al.,* 2019). In addition, miRNAs have a possibility to influence delivery processes (Menon *et al.,* 2017; Williams *et al.,* 2012) presented the existence of placenta-derived miRNAs and the possibility of miRNAs in the signaling from the fetal membrane to the uterus, especially in the mechanism of birth induction. Menon et al. (2019) identified that specific miRNAs significantly increased in human maternal blood at the late pregnancy period (Menon *et al.,* 2019). We focused on several possible miRNAs from Menon's study as a potential mediator in the mouse pregnant exosomes.

In this study, we examined the kinetic changes of EVs and exosomes in the circulating blood of pregnant mice and identified the appropriate tetraspanin marker that exhibits

consistency with exosome appearance. Using the tetraspanin marker, the localization of exosomes in mouse placenta tissues was confirmed. Furthermore, we found elevation of miRNAs in the mouse pregnant serum and discussed their functions.

2.3. Materials and Methods

2.3.1. Laboratory animals

ICR mice purchased from Japan SLC (Hamamatsu, Japan) were bred under the temperature 22 ± 2°C and 12–12 hr light-dark cycle with water and food *ad libitum*. Virgin female mice were paired with male mice in the evening and the females that vaginal-plug confirmed in the next morning were designated as gestational day 0.5 (Gd 0.5). Under inhalation anesthesia with isoflurane, more than 1 mL of blood was collected from the heart, and the mice were euthanized by cervical dislocation. Implantation sites were collected from the pregnant uterus. The serum was separated from the total blood by centrifugation. More than three pregnant mice were used from each pregnant day. Experimental designs using mice were preliminary reviewed and approved by the Ethical Committee on Animal Experimentation at Yamaguchi University (Approval numbers: 476 and 552).

2.3.2. Isolation of extracellular vesicles (EVs)

Cell debris was removed from the serums by additional centrifugation in 2,000 × g for 30 min at 4°C. The supernatants were incubated with the Invitrogen Total Exosome Isolation reagent (Thermo Fisher Scientific, Waltham, MA, U.S.A) at 2–8°C for 30 min. The pellets including EVs were collected by centrifugation in 10,000 × g for 10 min at room temperature.

2.3.3. Nanoparticle-tracking assay (NTA)

The EV pellets were suspended with cold phosphate buffer saline (PBS) that was filtered before with the membrane filter (0.22 μm). Samples were cryopreserved at -20 °C and sent to Quantum Design Japan (Tokyo, Japan) for the commission of particle analyses using NanoSight

NS300 (Malvern Panalytical, Malvern, U.K.). Samples were diluted with filtered PBS and measured five times regarding particle sizes and numbers. Data were averaged and converted by dilution rates. Gating was performed at the specified range of 30–150 nm particle sizes to detect the exosomes.

2.3.4. Transmission electron microscopy (TEM)

Purified exosomes were fixed with 4% paraformaldehyde for 10 min at room temperature. Suspended samples were mounted on the 200 nm meshes with the 20 nm-thickness carbon membrane attached (EM Japan, Tokyo, Japan). The meshes were fixed again with 1% glutaraldehyde for 5 min, rinsed with filtered PBS, and stained with 1% uranyl acetate for 5 min. After drying overnight at room temperature, the meshes were observed using an H-7100 electron microscope (Hitachi High-Technologies, Tokyo Japan).

2.3.5. Immunohistochemistry (IHC)

The tissue samples were fixed with 10% neutral-buffered formalin, and the implantation sites were trimmed out and cut through the median line of the placenta. Paraffin blocks were prepared by conventional procedures, and the sections were deparaffinized using xylene and subsequently hydrated by sequential treatment with 100 to 70% ethanol and distilled water. Antigen retrieval was performed on the section with Tris buffer pH 6.0 at 121°C for 15 min. Following a blocking process with 10% goat serum, sections were incubated at 4°C overnight with each primary antibody; anti-CD9, CD63, and CD81 (Abcam, Cambridge, MA, U.S.A). For negative control, tissue sections were incubated with PBS instead of primary antibody. After washing with PBS, sections were treated with 0.3% H_2O_2 for 15 min, and incubated with the Histofine Simple Stain Mouse MAX-PO (R) kit (Nichirei, Tokyo, Japan). The peroxidase reactivity was detected using the Peroxidase Stain DAB Kit (Nacalai Tesque, Kyoto, Japan), and counterstain was performed briefly with hematoxylin. Sections were observed using the conventional microscope (Nikon Eclipse CiE-E-31, Nikon, Tokyo, Japan) or the All-in-one

imaging system Mica (Leica Microsystems). Results of immunostaining were evaluated according to the immunoreactive score (IRS) by Remmele and Stegner (Popiel-Kopaczyk *et al.,* 2023). For score assessment, three fields were chosen at random at ×200 magnification and evaluated by two independent researchers. Two parameters were evaluated: (A) the percentage of positively stained cells in the field of view, which was scored as 0 = no positive cells, 1 = <10%, 2 = 10-50%, 3 = 51-80%, 4 = >80%, and (B) the staining intensity, which was scored as 0 = no color reaction, 1 = weak, 2 = moderate, 3 = strong. The final product of these two parameters (A×B) was compared (Figure 2.1).

2.3.6. Western blot

Purified EV pellets were suspended with the filtered cold PBS and mixed with proteolytic inhibitor (eComplete mini, EDTA-free, Roche, Manheim, Germany). Protein concentrations were measured by NanoDrop 2000 (Thermo Fisher Scientific), and adjusted to 40 mg/mL by the Laemmli Sample Buffer (Bio-Rad, Hercules, CA, U.S.A.) with 2-mercaptoethanol. Samples were denatured at 90°C for 10 min, and electrophoresed using 4-12% Invitrogen Bolt Bis-Tris Plus gel (Thermo Fisher Scientific). Transblotting was performed using polyvinylidene difluoride (PVDF) membranes (Merck KGaA, Darmstadt, Germany) and a transfer device (ATTO Blotting System, Tokyo, Japan). The membranes were treated with 5% bovine serum albumin for 30 min, and reacted with the primary antibody (Table 1) at 4°C overnight. The membranes were reacted with a horseradish peroxidase-conjugated secondary antibody at room temperature for 1 hr. The chemiluminescence reaction was initiated with ECL Pro western blotting Detection Reagent (PerkinElmer, Waltham, MA, U.S.A.) and detected using Amersham ImageQuant 800 (Cytiva, Tokyo, Japan). Images of western blotting were analyzed using Image J software (NIH, Bethesda, MD, U.S.A.). The quantified data were corrected by the protein concentration of each sample.

Western blot analysis of mouse serum was performed using the same techniques as for the samples of EVs. PVDF membranes were treated with specific antibodies: anti-CD63 and anti-syncytin-1 (Table 2.1). Syncytin-1 is a cell fusion protein, and the mouse trophoblasts show syncytin-associated cell fusion during placentation. Syncytin-1 is a marker for syncytiotrophoblasts (Vargas *et al.,* 2014).

Table 2.1. Primary and secondary antibodies used in western blot and immunohistochemistry

Application	Antibody names	Clonality	Immunogen	Catalogue No.	Manufacture	Dilution
Primary antibody	Anti-CD9	Rabbit polyclonal	Mouse	ab92726	Abcam	WB 1:2,500 IHC 1:500
	Anti-CD63	Rabbit polyclonal	Mouse	ab134045	Abcam	WB 1:2,500 IHC 1:2,000
	Anti-CD81	Rabbit polyclonal	Mouse	ab109201	Abcam	WB 1:2,500 IHC 1:700
	Anti-syncytin-1	Rabbit polyclonal	Human, mouse	bs-2962R	Bioss	WB 1:500
	Anti-mouse IgG	Rabbit polyclonal	Mouse	A90-217A	Bethyl Lab	WB 1:1,000
Secondary antibody	Anti-Rabbit IgG (H+L), HRP Conjugate	Donkey polyclonal	Rabbit	W-4018	Promega	WB 1:2,500

WB: western blot
IHC: immunohistochemistry

2.3.7. Detection of microRNA (miRNA)

The total RNA included in serum EVs was isolated using Total Exosome RNA and Protein Isolation Kit (Thermo Fisher Scientific), and then reversely transcribed to cDNA using Mir-X miRNA First-Strand Synthesis Kit (Takara Bio, Shiga, Japan). Real-Time PCR was performed in triplicate by using TB Green Advantage qPCR Premix (Takara Bio) on the CFX96 detection system (Bio-Rad). We selected the target miRNAs that increase in human blood from late pregnancy to term birth (Menon *et al.,* 2019), and the same miRNA sequences in mice were examined in the database of miRbase (https://mirbase.org). The forward primers were designed by replacing uracil with thymine in the miRNA sequences (Table 2.2). The sequence for U6 small nuclear (U6sn) RNA was used as a positive control. The forward primer for U6sn RNA and the universal reverse primer were provided by the manufacturer (Takara Bio).

Quantification PCR (qPCR) analysis was conducted on the ΔΔCt method. The relative amount of miRNAs was statistically compared between non-pregnant and Gd 18.5.

Table 2.2. Primer sequences for qPCR

Targets	Accession No.	Forward primers (5'-3')
mmu-miR-10b-3p	MIMAT0004538	CAGATTCGATTCTAGGGGAATA
mmu-miR-25b-3p	MIMAT0000652	CATTGCACTTGTCTCGGTCTGA
mmu-miR-143-3p	MIMAT0000247	TGAGATGAAGCACTGTAGCTC
mmu-miR-379-3p	MIMAT0017080	TATGTAACATGGTCCACTAACT

2.3.8. Statistical analysis

All data were presented as means ± standard deviation, with n=3 different samples per group. For comparisons between two groups, the two-sample *t*-test was performed when equal variance was detected by the preliminary F-test. When unequal variance was detected, the Welch *t*-test was performed. For multi-group comparisons, analysis of variance (ANOVA) was used. Statistical differences between groups were identified by *post-hoc* analyses with Tukey's Honest significant test. Statistical significance was defined as at least $P<0.05$.

2.4. Results

2.4.1. Dynamics of the exosomes in the pregnant serum

In the mouse serum at non-pregnant and gestational periods, a number of EVs were present (Fig. 2.2A-E). The concentration of EVs increased continually after Gd 10.5, and the diameter decreased at Gd 14.5 and 18.5 compared to non-pregnant (Table 2.3). These dynamics appeared to be due to variations in the exosomes in the EVs. Exosomes were distinguished from the sizes between 30 and 150 nm (Figs. 2.2A-E). From non-pregnant to Gd 10.5, the percentage of exosomes in EVs was about 50%, however, they increased rapidly to 80.1% at Gd 14.5 (Table 2.3). At 18.5 days, most of the EVs in serum were composed of exosomes (97.5%). Concentrations of exosomes were increased drastically at Gd 14.5 and Gd 18.5 days, reaching 2.86 and 13.5 times more than non-pregnant. TEM observation found the two types of EVs

(Figs. 2.2F, 2.2G), and the large-sized EVs were spherical or oval shapes and the shortest diameter was more than 200 nm. These large-sized EVs were considered microvesicles according to the size classification (Nair and Salomon, 2018) and they were frequently observed in the serum of non-pregnant, Gd 6.5, and 10.5. The exosomes in mouse serums showed a consistent size and morphology. Observations at Gd 14.5 and 18.5 showed a dominance of exosomes with few microvesicles. At the serum of Gd 18.5, significantly small-sized exosomes were observed (Table 2.4).

Table 2.3. Measurements of extracellular vesicles (EVs) in mouse serums

	Non-pregnant	Gd 6.5	Gd 10.5	Gd 14.5	Gd 18.5
Concentration of total EVs in serum ($x10^{10}$/mL)	12.4 ± 0.79^{a}	14.3 ± 0.18^{a}	19.5 ± 0.42^{b}	22.8 ± 0.17^{c}	86.9 ± 5.43^{d}
Average EVs diameter in serum (nm)	158.8 ± 2.1^{e}	167.6 ± 1.0^{f}	163.5 ± 2.0^{f}	127.6 ± 1.6^{g}	71.2 ± 1.6^{h}
Rate of sEVs in total EVs	53%	43.6%	47.5%	80.1%	97.5%

[a-h] Significant differences were found between the different alphabet. $P<0.01$

Table 2.4. Properties of serum sEVs and expression of microRNA

	Non-pregnant	Gd 6.5	Gd 10.5	Gd 14.5	Gd 18.5
Calculated concentration of sEVs in serum ($x10^{10}$/mL)[1]	6.33 ± 1.26^{a}	6.35 ± 0.06^{a}	9.10 ± 0.19^{b}	18.16 ± 1.22^{c}	85.61 ± 1.2^{d}
Average sEVs diameter in serum (nm)	138.07 ± 7.83^{e}	140.17 ± 13.23^{e}	140.97 ± 12.6^{e}	125.6 ± 2.78^{e}	69.97 ± 1.85^{f}
qPCR detection of microRNAs in serum EVs[2]					
miR-10b-3p	1.00 ± 0.983	—	—	—	9.49 ± 3.25**
miR-25b-3p	1.00 ± 0.745	—	—	—	17.0 ± 7.90*
miR-143-3p	1.00 ± 0.206	—	—	—	19.5 ± 8.79*
miR-379-3p	1.00 ± 1.00	—	—	—	1.54 ±1.35

[1]Calculated from the data of Table 2
[a-f] Significant differences were found between the different alphabet. $P<0.01$
[2]Quantification results were displayed relatively to the amount of Non-pregnant as 1.00.
*$P<0.05$, **$P<0.01$, vs. Non-pregnant

2.4.2. Western blots by tetraspanin markers and syncytin-1

The tetraspanin markers (CD9, CD63, and CD81) showed different positive patterns on the EV samples during gestational periods (Fig. 2.3A). Quantitative analyses showed that the amount of CD9 did not fluctuate statistically from Gd 6.5 to 14.5 and decreased at Gd 18.5 (Fig. 2.3B). CD63 showed little change from Gd 6.5 to 10.5, and gradually increased after Gd 10.5 (Fig. 2.3C). The decreasing tendency was remarkable on CD81 from non-pregnant to Gd 10.5 (Fig. 2.3D). Of these results, the quantitative changes in CD63 were most similar to the fluctuation of exosome concentrations during gestation (Table 2.3). Serum at Gd 12.5, which corresponds to the period of active placentation, also showed a positive reaction for CD63 and syncytin-1 (Fig. 2.3E). This reaction disappeared when the EVs were removed from serums. Reactivity to syncytin-1 also disappeared when EVs were depleted from serum. Furthermore, syncytin-1-positive EVs were specific on the serum from the gestational periods (Fig. 2.3F), showing that anti-syncytin-1 has the potential to detect the serum EVs derived from STs.

2.4.3. Detection of exosomes in mouse placentas

With a color development time of 1.5 min by DAB, the anti-CD63 antibody showed strong reactivity at the mouse placenta (Fig. 2.4B). At the same coloration time, anti-CD9 and anti-CD63 antibodies showed weak and moderate reactivity (Fig. 2.4A and 4C, respectively). These results are in accordance with the scoring evaluation (Fig. 2.1).

Immunoreactivity for CD63 was obvious at the placental labyrinth region, the area for material exchanges between dams and fetuses. High-resolution images showed precise localization of CD63 at the cell membrane of STs (Fig. 2.4E). Dot-like reactivities were also present in the cytoplasm. CD63-positive reactions were also observed on the membrane of endothelial cells of fetal capillaries.

2.4.4. Detection of miRNA in mouse serum-derived EVs

EV samples from mouse serum were analyzed for the contents of miRNAs (Table 2.3). EVs at Gd 18.5 contained significantly higher amounts for miR-10b-3p, 25b-3p, and 143-3p, compared to those of non-pregnancy. Besides that, miR-379-3p showed an increased tendency at Gd 18.5, but no significant difference was confirmed compared to non-pregnancy.

2.5. Discussion

This study shows the variation of EVs in the serum of non-pregnant and pregnant mice. Exosomes accounted for more than half of EV composition, and the appearance of exosomes seemed to be the major factor of EV variation during pregnancy. Exosomes increased rapidly after Gd 14.5, which corresponded to the completion period of mouse placentation. Exosomes in mouse serums increased most before parturition, a finding consistent with previous reports (Nguyen *et al.,* 2019; Sheller-Miller *et al.,* 2019b).

Of the detection patterns for tetraspanin markers, CD63 was consistent with exosome variation in the pregnant serums. CD63 seemed to be a useful marker for detecting exosomes among other tetraspanin markers. Since tetraspanins are also present in the microvesicles, it would be difficult to completely identify only exosomes. However, microvesicles are formed by the budding process at the cell surface, while exosomes are formed through the cytoplasmic endosomes (van Niel *et al.,* 2018). Positive reactions for CD63 were found on the cell membranes of both STs and epithelial cells. It is not known whether these reactions are indicative of exosomes forming near the membrane, accumulating just below the membrane, or what state they are in. The dotted reactivities in the cytoplasm are possible to indicate endosomes, a preliminary stage of exosomes. The study of human pancreatic malignant tissue also showed membranous and dotted images for the immunostaining of CD63 (Khushman *et al.,* 2017). They described the limitations for the precise observation of exosomes due to low

resolution with optical microscopy, including confocal microscopy. Immunoelectron microscopic analysis would be necessary to determine what is reacting positively.

In any case, the CD63-positive reactions indicated the possibility that exosomes are produced in both STs and epithelial cells and are secreted into both maternal and fetal blood. This result is consistent with the reports for exosome distribution cells in human placentas (Mitchell *et al,* 2015). STs form a placental barrier between fetal and maternal blood and contribute to the selective transport of substances. The other of our results, CD63-positive reaction in the fetal endothelial cells, is of a localization not known in human placentas. Endothelial cells act as the interface between circulating blood and tissues. They have important roles in controlling oxygen exchange, nutrients, and cellular trafficking (Ricard *et al.,* 2021). Endothelial cells are found to produce a significant proportion of the EVs found in blood (de Jong *et al.,* 2012; Mathiesen *et al.,* 2021). It has been demonstrated that endothelial cells can also be targeted by exosomes derived from STs to alter gene expression (Cronqvist et *et al.,* 2017). Since the inner layer of STs is in contact with the fetal capillaries, there is potential for molecular communication between STs and endothelium via exosomes.

Circulating levels of maternal exosomes increase in humans and placenta-specific miRNAs have been identified (Menon *et al.,* 2019). Stefanski *et al*. (2019) showed that the exosomes including specific miRNAs are released by mouse trophoblasts, which are abundant in the serum of pregnant mice (Stefanski *et al.,* 2019). Of the four miRNAs that are increased in the human placenta (Menon *et al.,* 2019), we found three of them were also increased in the EVs of mouse pregnant serums. This increase was in response to the increase of serum exosomes. miR-10b-3p, miR-25b-3p, and miR-143-3p have a possibility to have a physiological role in normal pregnancy.

MiR-10b-3p has been found in the placentas of patients with preeclampsia (PE) (Zhu *et al.,* 2009). In mice also, mir-10b-3p is found in the PE model, suggesting an effect on

trophoblasts for their viability, migration, and invasion (Li *et al.,* 2019). In humans, mir-10b-3p is proposed to regulate inflammatory responses, migration, and proliferation in the trophoblasts under hypoxia conditions, by targeting the mRNA for lipopolysaccharide (LPS)-induced tumor necrosis factor α factor (LITAF) (Li *et al.,* 2019).

Under normal pregnancy conditions, human placentas can transport miR-25-3p containing EVs to the myometrium and inhibit excessive expression of Ca^{2+} pump protein (Wang *et al.,* 2021). This effect is considered to maintain the calcium homeostasis in the myometrium and contribute to avoiding preterm birth. On the other hand, miR-25b-3p is suggested for adverse pregnancy outcomes including hypertensive disorders, fetal growth restriction, and preterm birth (Loscalzo *et al.,* 2021; Wang *et al.,* 2021; Zhou *et al.,* 2022).

In pigs, miR-143-3p was isolated from EVs in the uterine luminal fluids (Ding *et al.,* 2022). Furthermore, knockdown of miR-143-3p in mice led to failure of embryo implantation. Studies in humans revealed that miR-143-3p regulates adipogenic growth in pregnancy by targeting MAPK-activated protein kinase 5 (Cheng *et al.,* 2014; Zhang *et al.,* 2016). This effect is considered to prevent excessive fetal growth. miRNAs may have similar effects across animal species if the target gene sequences are similar. In this study, physiological functions of miR-25-3p and miR-143-3p were suggested to be also at work at the late and end pregnancy periods in mice, for example in parturition or fetal growth.

Moreover, this study found the size reduction of exosomes at Gd 18.5. Exosomes are divided into the following subpopulations according to their sizes: exomeres (~35 nm), Exo-S (60–80 nm), and Exo-L (90–120 nm) (Zhang *et al.,* 2018). Mouse exosomes were predicted to be predominantly Exo-L at non-pregnant, Gd 6.5, 10.5, and 14.5, and to convert to Exo-S at Gd 18.5. The proteome analyses showed that the cargo proteins in Exo-L were rich in those involved in IL-2/STAT5 signaling and immunomodulation pathways (Zhang *et al.,* 2018). It is known that IL-2/STAT-5 signaling is associated with an increase of regulatory T (Treg) cells

during early pregnancy (Fainboim and Arruvito, 2011), which suppress maternal allogeneic responses directed against the fetus. Aluvihare *et al.* (2004) also reported the depletion of Treg cells leads to failure of pregnancy. Especially during the period of implantation and early placentation, when the contacts between endometrium and embryos begin and strengthen, the Treg effect by Exo-L may be necessary for the establishment of pregnancy.

Taken together, our study showed that mouse serum EVs were mainly composed of exosomes and they were derived from the completed placentas. The CD63 tetraspanin marker is useful in identifying the dynamics and localization of mouse exosomes. Immunostaining of CD63 provided a new finding for the exosomal localization in the mouse placenta. Several miRNAs encapsulated in exosomes were present in maternal serum at Gd 18.5 and involved in the physiology of normal pregnancy. These results will be useful in the studies of the normal pregnancy process, in the pathological analysis of human models of abnormal pregnancy, and in the development of monitoring molecules for pregnant failures.

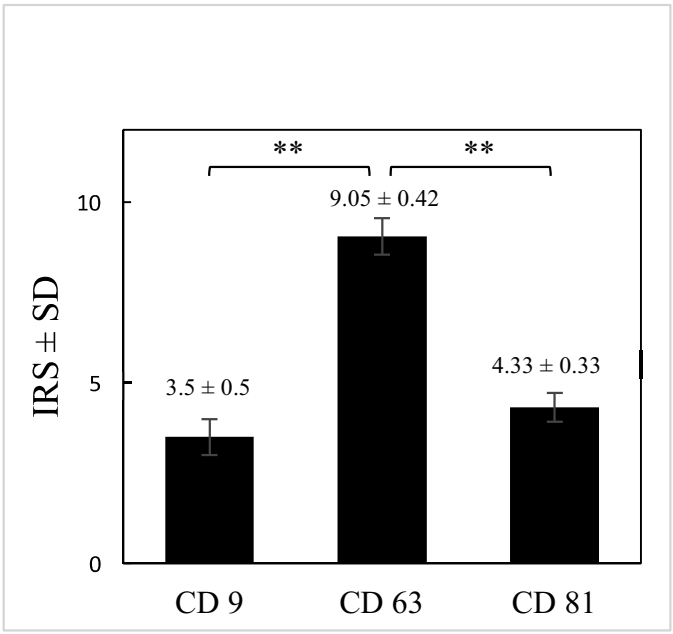

Figure 2.1. Evaluation of immunostaining for CD9, CD63, and CD81 in the labyrinth region at Gd 18.5 using immunoreactive score (IRS). ***P*<0.01

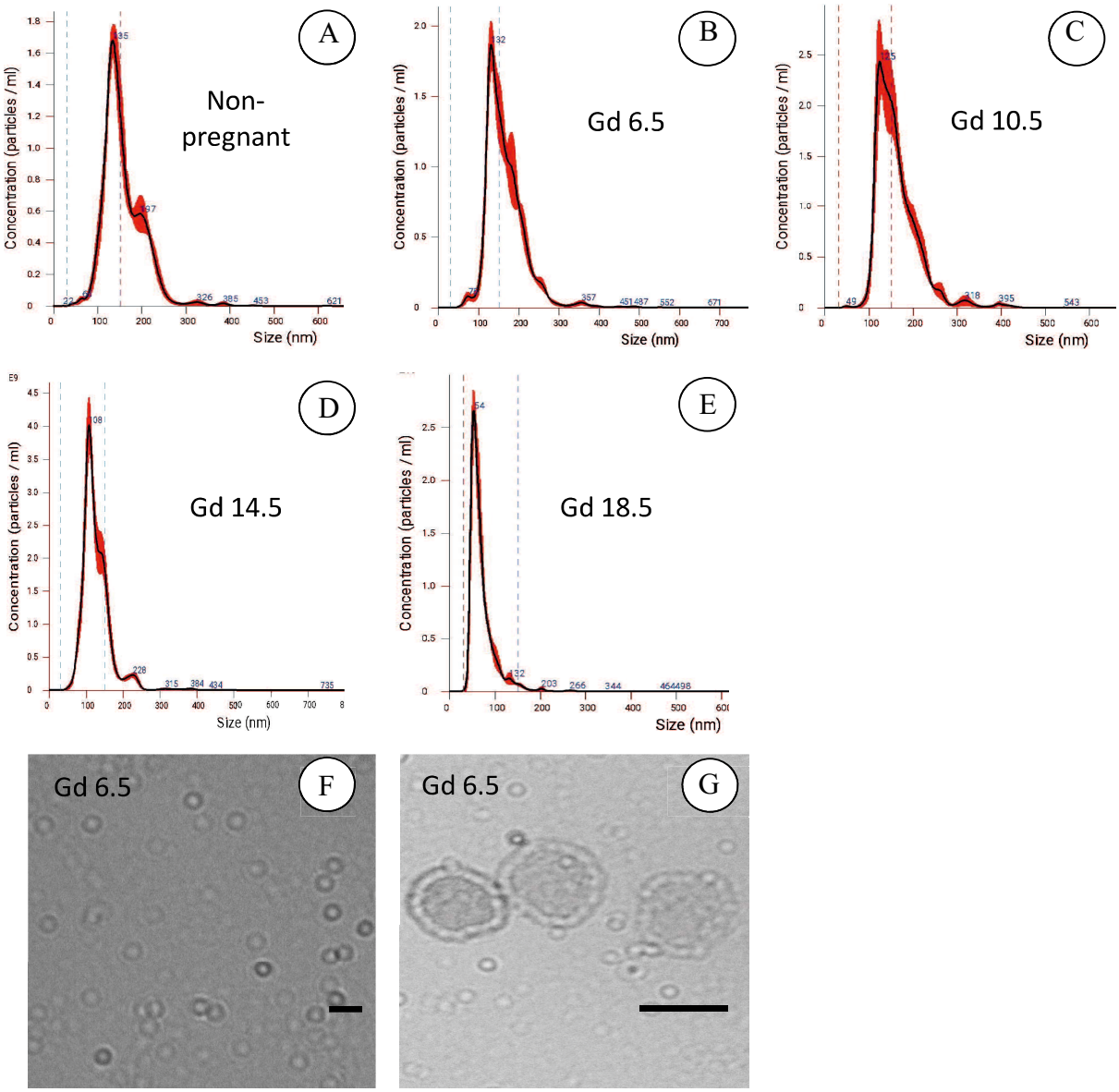

Figure 2.2. Results of nanoparticle-tracking assays for the extracellular vesicles (EVs) isolated from mouse serums at non-pregnant (NP) and several gestational days (Gd). Graphs of A-E show the distribution of EV diameters and dotted line areas represent ranges of the exosomes size 30-150 nm. F, G) Representative images for exosomes observed by TEM. At Gd 6.5, two types of EVs were seen. Size classification allows identification of the smaller one as exosomes (F, about 100 nm) and the larger one as microvesicles (G, more than 200 nm). Bar scales = 100 nm (F) and 250 nm (G).

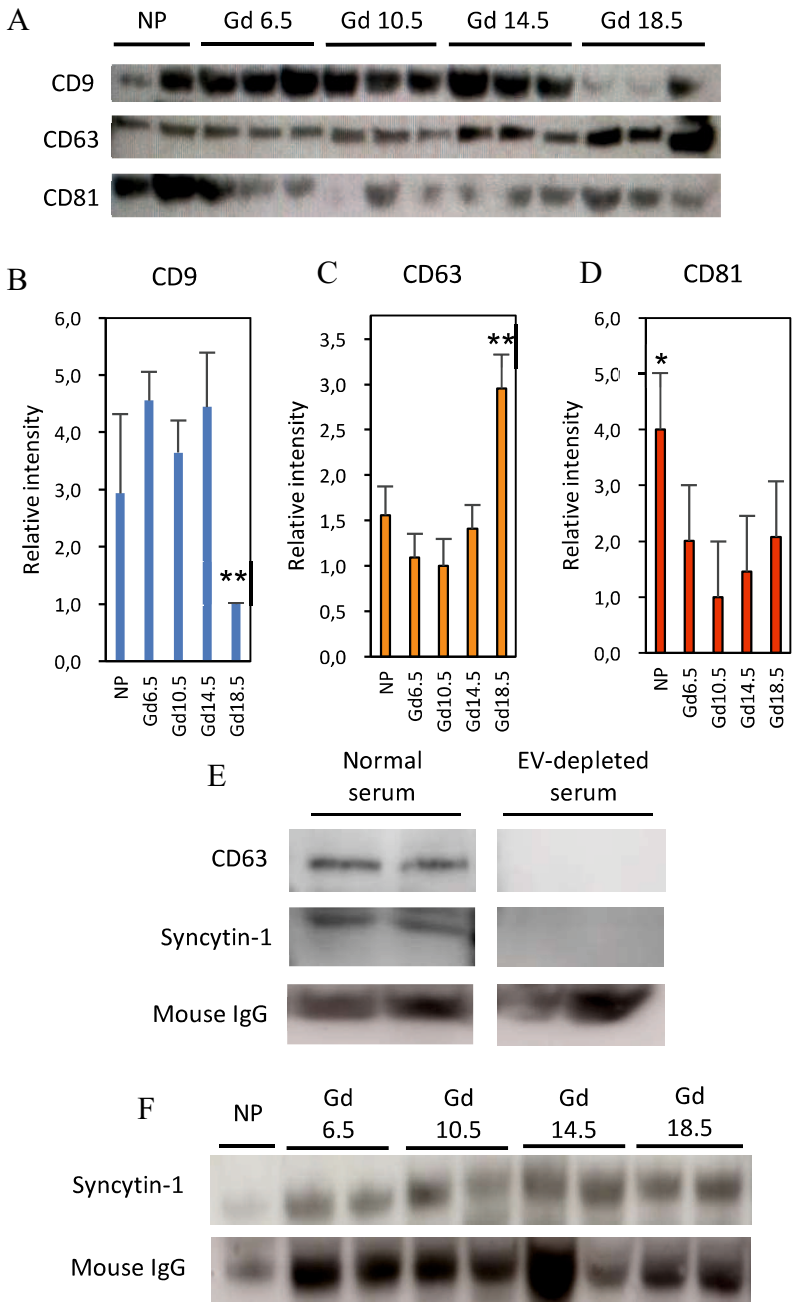

Figure 2.3. Western blot and quantitative analyses of isolated EVs. A) Western blot analysis of CD9, CD63, and CD81 were detectable on the EVs purified from the serums of non-pregnant (NP), gestational day (Gd) 6.5, 10.5, 14.5 and 18.5. B-D) Results of the quantitative analysis. For the analysis of CD9, Gd 18.5 was contrasted as 1.0 (B). There was a significant difference in detection at Gd 18.5 compared to Gd 6.5, 10.5, and 14.5. For CD63 (C), Gd 10.5 was contrasted as 1.0; there was a significant difference at Gd 18.5 compared to Gd 6.5, 10.5, and 14.5 as well as NP. For CD81 (D), Gd 10.5 was contrasted as 1.0; there was a significant difference at NP compared to Gd 10.5, and 14.5. $^{**}P<0.01$, $^{*}P<0.05$. (E) Western blot of normal serum at Gd 12.5 showed the positive bands for CD63 and also syncytin-1, a marker for the syncytiotrophoblasts. When EVs were depleted from the Gd 12.5 serum using an EV isolation reagent, positive reactivities for CD63 and syncytin-1 disappeared. Mouse IgG was used as a positive control. (F) The isolated EVs showed very low expression of syncytin-1 in the non-pregnant (NP) serum compared to those in the gestational day (Gd) 6.5-18.5. Mouse IgG was used for positive control.

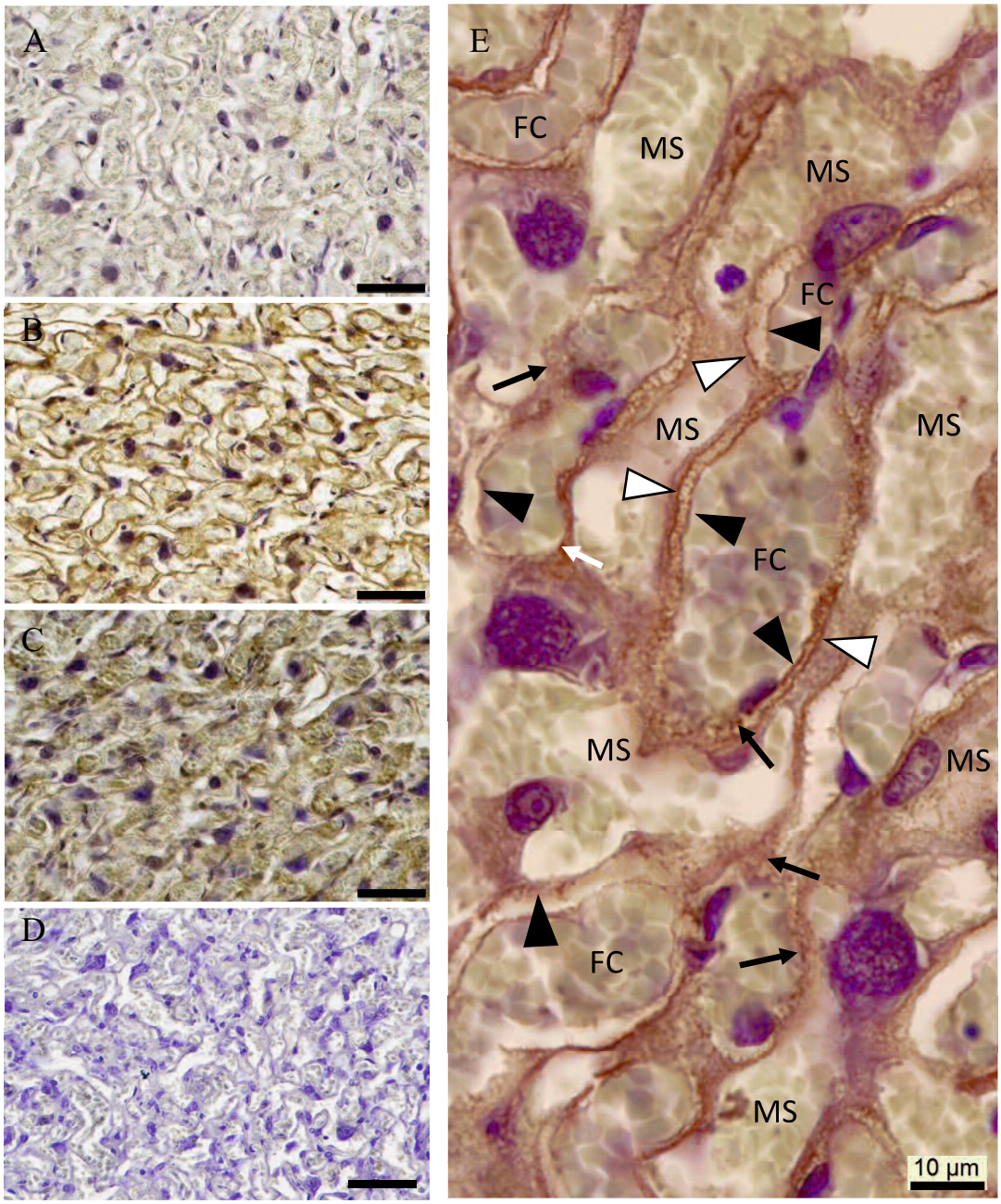

Figure 2.4. Immunohistochemical staining on the mouse placental tissues at Gd 18.5. The labyrinth area showed positive reactions for CD9 (A), CD63 (B), and CD81 (C). C) The strongest reactivity was seen to the anti-CD63 antibody. D) Negative control for A-C. E, F) The high-resolution images of the CD63 immunostaining. E) Positive reactions were identified in the cell membrane of syncytiotrophoblasts (white arrowheads) as well as the fetal endothelial cells (black arrowheads). The dot-like CD63-positive reactions are found in the cytoplasm of syncytiotrophoblasts (white arrows) and endothelial cells (black arrows). MS: maternal sinusoids, FC: fetal capillaries. Scale bars = 50 µm (A-D).

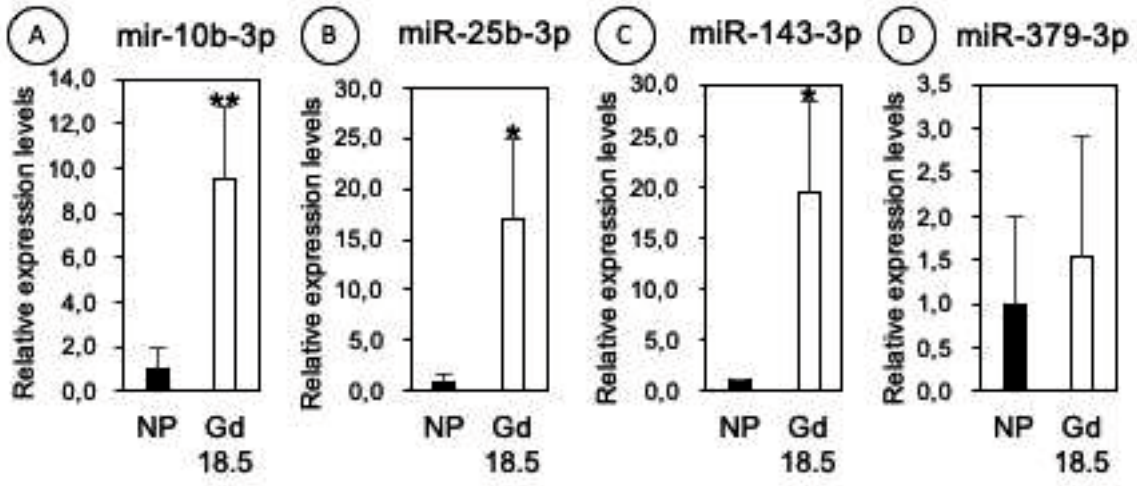

Figure 2.5. miRNAs in the serum EVs were detected by qPCR (A-D). NP: non-pregnant, Gd: gestational days. Quantification results are displayed relative to the amount of NP as 1.0. **P*<0.05, ***P*<0.01.

CHAPTER 3

Exosomes and their miRNA roles in an L-NAME-induced preeclampsia mouse model associated with angiogenesis

3.1. Abstract

Dysregulation of angiogenetic factors interfere with the normal progression of pregnancy and is a cause of preeclampsia (PE). In this study, we investigated the dynamics of exosomes and variations of physiological factors and micro RNA (miRNA) contained in exosomes on the pathogenesis of PE. A total of 18 pregnant-ICR mice were used in this study divided into two groups, i.e. healthy pregnancy (HP) as a control group and PE as an experimental group. In PE group, 50 g/kg BW/day of L-NAME was injected subcutaneous to pregnant mice start from gestational day (Gd) 7.5 to Gd 17.5, while PBS was applied to HP group. At Gd 17.5, mice were sacrificed and blood sample was collected for extracellular vesicles (EVs) examination, western blot, and RT-PCR. Then, fetus and placenta of mice were collected and fixed with 10% neutral buffered formaldehyde for histopathological and immunohistochemical evaluations. All variables were analyzed statistically using t-test (P<0.05). L-NAME administration induce PE-like phenotype showing hypertension, increased protein in urine, decreased fetal and placental weight, and histopathological changes in placenta. In PE group, we found a significant increase in exosome concentration. Protein expression of VEGF and iNOS in the placenta and serum-derives EVs from PE mice were higher compared to HP. We also validated the down-regulation of miR 16-5p and up-regulation of miR 25b-3p in PE mice. According to these results, increased expression levels of VEGF and iNOS encapsulated via exosomes, as well as dysregulation of exosomal miRNA (exomiR) play an important role in pathogenesis of PE.

3.2. Introduction

Preeclampsia is a condition marked by high blood pressure (BP) and protein in urine (Steegers *et al.,* 2010; James *et al.,* 2013). The cause of PE is still unknown, but it is believed to be caused by the invasive damage of placental trophoblast cells as they invade the maternal

decidua and spiral arteries (Makris *et al.*, 2007; North *et al.,* 1994). This damage lead to changes in the blood flow of the placenta, which can result in intra-uterine growth restriction (Karumanchi *et al.,* 2009). The proper development of the placenta depends on the coordination between the maternal decidua and fetal-derived cells, where angiogenic growth factors play a role in this process (Karumanchi *et al.,* 2009).

Extracellular vesicles (EVs) are small structures that originate from cells and come in different sizes and types, including exosomes (30-150 nm diameter), microvesicles (100-1000 nm diameter), and apoptotic bodies (1-10 μm diameter) (Zaborowski *et al.,* 2015; Yáñez-Mó *et al.,* 2015; Borges *et al.,* 2013). Recently, scientists have been interested in the role of exosomes that are secreted by placental cells in regulating cell-to-cell communication (Nakahara *et al.,* 2020). Exosomes are formed by the inward budding of late endosomes, and they are released into the extracellular space when they fuse with the plasma membrane (Zhang *et al.,* 2018). Once released, exosomes can travel to other cells and interact with them by delivering their contents, which can affect the physiological or pathological state of the cell (Wei *et al.,* 2021). The contents of exosomes are complex and include various types of proteins, RNAs, and DNAs that act as messengers for local and distant cell communication (Shao *et al.,* 2018). During pregnancy, the placenta expresses many essential protein and miRNAs, which can be packed in exosomes (Pillay *et al.,* 2016; Gill *et al.,* 2019). Under stressful conditions, such as PE, more exosomes are shed from the placenta into the maternal circulation (Matsubara, 2023). The release of EVs into the maternal bloodstream has also been observed to correlate with systolic blood pressure in cases of PE (Lok *et al.,* 2008). This suggests that increased levels of EVs in maternal circulation may cause the symptoms associated with PE.

Vascular endothelial growth factor (VEGF) as an angiogenic growth factor is known to regulates vascular permeability (Lal *et al.,* 2001; Bates *et al.,* 2010), which are commonly observed in PE. Different results occur regarding the VEGF concentration measured in the

maternal circulation during normal and PE pregnancies (Kurbanov *et al.,* 2018; Mochan *et al.,* 2019). Furthermore, VEGF stimulates the release of nitric oxide (NO), a vasodilator, and regulates the expression of nitric oxide synthase (NOS) (Kroll and Waltenberger, 1998; Hood *et al.,* 1998; van der Zee *et al.,* 1997). It has been established that endothelial NOS (eNOS) and inducible NOS (iNOS) are present in several mammalian placentas (Khan *et al.,* 2012; Purcell *et al.* 1997). A previous report shows that placental trophoblast-EVs in women with PE have reduced levels of eNOS, resulting in decreased production of NO. This suggests that EVs may contribute to decreased NO bioavailability. However, there are currently limitation reports on iNOS expression in PE associated with EVs.

Furthermore, the role of NOS was clarified through experiments involving the systemic administration of a competing NO inhibitor, L-N^G-Nitro-arginine methyl ester (L-NAME) (Liu *et al.,* 2019). This inhibitor can also be used to simulate preeclampsia (Motta et al., 2005; de Alwis *et al.,* 2022). Therefore, in this study, we aim to investigate whether L-NAME administration exhibits a PE phenotype and observe the pathological changes in the placenta under PE-like conditions. We will also characterize maternal exosome circulation in the serum of PE mice induced by L-NAME and examine the protein expression of VEGF and iNOS in the placenta tissue and serum-derived EVs from HP as compared to those with PE. Additionally, our previous report showed the variation of the miRNAs expression through normal pregnancies suggested their involvement in normal physiological pregnancy processes (Yustinasari et al., 2024). In this study, we identified several miRNAs (miR 126a-3p, miR 16-5p, miR 10b-3p, and miR 25-3p) isolated from serum derived-EVs that contribute to the pathogenesis of PE and describe their role.

3.3. Materials and Methods

3.3.1. Laboratory animals

Eighteen-female ICR mice, aged eight weeks, were purchased from Japan SLC located in Hamamatsu, Japan. The mice were housed in the experimental animal facilities at Yamaguchi University, where they were kept under standard conditions at a temperature of 22 ± 2°C, with a controlled 12-hour light/dark cycle. They had free access to standard food and water. Female mice were mated with male mice in the evening, and those females that had a vaginal plug confirmed the following morning were designated as gestational day (Gd) 0.5.

Pregnant mice were randomly allocated into two treatment groups. The healthy pregnancy (HP) group, which served as the control group (n=9), was given phosphatase buffer saline (PBS) daily. The preeclampsia (PE) group (n=9) was administered L-NAME (50 mg/kg BW/day; Sigma-Aldrich) (Motta et al., 2015; de Alwis et al., 2022). All treatment was injected via 100 ul subcutaneous injection from Gd 7.5 to Gd 17.5 (approximately early second trimester to term in human equivalent to model early onset disease).

Before experimentation, mice were acclimated to the CODA non-invasive blood pressure system (Kent Scientific) in a seven-stage process involving exposure to the restraining tube and tail cuff. Then, tail blood pressure was measured and urine was collected at various points during gestation. On Gd 17.5, the mice were euthanized with isoflurane in oxygen, and cardiac puncture performed to collect maternal blood. Mice were then culled by cervical dislocation. Blood samples were allowed 20 minutes to coagulate at room temperature before centrifugation to separate the serum. Fetuses and placentas were also collected, weighed, and fixed in 10% neutral buffered formalin. Formalin-fixed tissue was embedded in paraffin and sectioned on a microtome for examination of structural changes. The animal procedures were approved by the ethical committee on animal experimentation at Yamaguchi University (Approval number: 476 and 552).

3.3.2. Isolation of extracellular vesicles (EVs)

Approximately one milliliter of mouse maternal blood was collected via intracardiac puncture at Gd 17.5. The collected samples were incubated at room temperature for 20 minutes and then centrifuged at 2000× g at 4 ◦C for 30 minutes. The serums were cleared of cell debris by additional centrifugation at 2,000 × g for 30 minutes at 4°C. The supernatants were then incubated with the Invitrogen Total Exosome Isolation reagent (Thermo Fisher Scientific, Waltham, MA, U.S.A) at 2–8°C for 30 minutes. Finally, the pellets containing EVs were collected by centrifugation at 10,000 × g for 10 minutes at room temperature. Purified EVs were analyzed for size and concentration using a nanoparticle imaging analyzer (Videodrop, Myriade, France).

3.3.3. Transmission electron microscope (TEM)

Purified EV samples were fixed with 4% paraformaldehyde for 10 min at room temperature. Ten μL of suspended samples were loaded on the grid with a 20 nm carbon membrane (EM Japan, Tokyo, Japan), incubated for 20 min, and fixed again with 1% glutaraldehyde for 5 min. After rinsing with a drop of 10 μL filtrated PBS, grids were stained with 1% uranyl acetate for 5 min. After drying overnight at room temperature, the grid was then placed in a specimen holder of H-7100 electron microscope (Hitachi, Tokyo Japan). The images were captured at × 15,000–30,000 magnification.

3.3.4. Immunohistochemistry (IHC)

The placenta samples were fixed in 10% neutral-buffered formalin and then embedded in paraffin. Sagittal transverse placenta sections that were 6-μm-thick were prepared, mounted on glass slides, and allowed to dry. They were then deparaffinized, and antigen retrieval was performed on the section with Tris buffer pH 9.0 at 121°C for 15 minutes. Following a blocking process with 10% goat serum, the sections were incubated at 4°C overnight with each primary antibody at indicated dilutions as follows: anti-VEGF, anti-iNOS, anti-CD63, anti-CD81, and

anti-syncytin. Then, the sections were treated with 0.3% H2O2 for 15 minutes and incubated with the Histofine Simple Stain Mouse MAX-PO (R) kit (Nichirei, Tokyo, Japan) for one hour at room temperature. The peroxidase reactivity was detected using the Peroxidase Stain DAB Kit (Nacalai Tesque, Kyoto, Japan). Finally, the sections were lightly counterstained with hematoxylin before being dehydrated, cleared, and mounted. The same steps were followed without the primary antibodies for negative controls, and no staining was observed. The sections were observed using the light microscope (Nikon Eclipse CiE-E-31, Nikon, Tokyo, Japan) or the all-in-one imaging system Mica (Leica Microsystems). To count the expression of VEGF, iNOS, and CD63, quantification was carried out by two researchers using an immuno reactive score (IRS) method by Remmel. Two center areas in the labyrinth from 18 different samples for each group were selected. Images were captured and obtained with Nikon imaging software (NIS).

3.3.5. Western blot (WB)

Exosome samples were quantified using Nano Drop 2000 (Thermo Fisher Scientific), and the absorbance was measured at 280 nm. After quantification, 40 µg of total protein was loaded into each well by adding 2x Laemmli Buffer with ß-mercaptoethanol. The samples were then heated on a block incubator (Astec, Japan) at 95◦C for 5 minutes for protein denaturation. Electrophoresis was performed using 4-12% Invitrogen Bolt Bis-Tris Plus gel (Thermo Fisher Scientific) and a molecular weight marker (BlueStar Prestained Protein Marker from Nippon Genetics, MWP03) was used. An electric current was applied to the electrophoresis cuvette with running buffer. Proteins were then transferred to a polyvinylidene difluoride (PVDF) membranes and transfer device (ATTO Blotting System, Tokyo, Japan). Subsequently, membranes were blocked with BSA 5% for 30 min. Finally, the membranes were incubated with the primary antibody (Supplementary Table 1) overnight at 4◦C. The next day, the membranes were reacted with a horseradish peroxidase-conjugated secondary antirabbit

antibody at room temperature for 1 hr. The chemiluminescence reaction was initiated with ECL Pro western blotting Detection Reagent (PerkinElmer, Waltham, MA, U.S.A.) and detected using Amersham ImageQuant 800 (Cytiva, Tokyo, Japan). Densitometric analysis was performed to determine the intensity of the bands using the Image J software (NIH, Bethesda, MD, USA). The intensity values obtained from the quantification were normalized using CD81, an exosome marker, of each sample.

Table 3.1. Primary and secondary antibodies used in immunohistochemistry and western blot

Application	Antibody names	Clonality	Immunogen	Catalogue No.	Manufacture	Dilution
Primary antibody	Anti-VEGF	Rabbit polyclonal	Mouse	sc-507	Santa Cruz Biotech	IHC 1:500 WB 1:1,000
	Anti-iNOS	Rabbit polyclonal	Mouse	sc-650	Santa Cruz Biotech	IHC 1:500 WB 1:1,000
	Anti-CD63	Rabbit polyclonal	Mouse	ab134045	Abcam	WB 1:2,500
	Anti-CD81	Rabbit polyclonal	Mouse	ab109201	Abcam	WB 1:2,500
	Anti-syncytin-1	Rabbit polyclonal	Human, mouse	bs-2962R	Bioss	WB 1:500
Secondary antibody	Anti-Rabbit IgG (H+L), HRP Conjugate	Donkey polyclonal	Rabbit	W-4018	Promega	WB 1:2,500

IHC: immunohistochemistry
WB: western blot

3.3.6. Detection of microRNA (miRNA) by Real-Time PCR

The Total Exosome RNA and Protein Isolation Kit (Thermo Fisher Scientific) was used to isolate the total RNA in serum EVs. Then, it was reversely transcribed to cDNA using the Mir-X miRNA First-Strand Synthesis Kit (Takara Bio, Shiga, Japan). Real-Time PCR was conducted in triplicate using TB Green Advantage qPCR Premix from Takara Bio on the CFX96 detection system (Bio-Rad). We selected four miRNAs based on literature review, namely miR 126a-3p, which extensively studied in the context of PE; miR 16-5p, which known as targeting VEGF; and the little-studied of miR 10b-3p and miR 25-3p. miRNA sequences in mice was confirmed at the miRbase database (https://mirbase.org). The forward primers were designed by replacing uracil with thymine in the miRNA sequences (Table 3.2). The sequence

for U6 small nuclear (U6sn) RNA was used as a positive control. The forward primer for U6sn RNA and the universal reverse primer were provided by the manufacturer (Takara Bio). Quantification PCR (qPCR) analysis was conducted using the ΔΔCt method. The relative expression of miRNAs was statistically compared between PE and HP groups at Gd 17.5.

Table 3.2. Primer sequences for qPCR

Targets	Accession No.	Forward primers (5'-3')
mmu-mir-126a-3p	MIMAT0004538	TCGTACCGTGAGTAATAATGCG
mmu-mir-16-5p	MIMAT0000652	TAGCAGCACGTAAATATTGGCG
mmu-mir-10b-3p	MIMAT0000247	CAGATTCGATTCTAGGGGAATA
mmu-mir-25-3p	MIMAT0017080	CATTGCACTTGTCTCGGTCTGA

3.3.7. Statistical analysis

Database management and statistical analyses of the variables were performed using Microsoft Excel. For descriptive statistics, means and standard deviations (SD) were used. Among the two experimental groups, an unpaired *t* test was performed when F-test indicated the equal variance, or the Welch t-test was conducted when unequal variance was confirmed. Statistical significance was defined as at least $P<0.05$.

3.4. Results

3.4.1. L-NAME administration to pregnant mice showed preeclampsia phenotypes

In PE mice, maternal hypertension elevated at Gd 17.5. Systolic BP reached 150 mmHg, whereas that in normal pregnant mouse remains around 115 mmHg. Diastolic BP at Gd 17.5 in PE mice reached 116 mmHg, whereas that in normal pregnant mouse remains around 81 mmHg (Figure 3.1A-B). In addition to hypertension, PE mice showed protein elevation in urine, which were elevated at Gd 17.5 as compare to HP (Figure 3.1C).

At the same gestational day, the weight of both the fetus and placenta were analyzed to assess the impact of L-NAME administration during pregnancy. The results showed that the

weights of fetus and placenta were significantly lower in the PE group compared to the healthy pregnancy groups ($P<0.05$) (Figure-1D). Macroscopically, fetus from PE group was smaller than HP group (Figure 3.1E).

3.4.2. Histopathological changing in preeclampsia mouse placenta

To clarify the relationship between L-NAME administration and placental dysfunction, we examined the pathological changes in the placenta under the condition of accelerating maternal hypertension using Haematoxylin and Eosin (HE) staining (Figure 3.2A-D). In fetoplacental region, particularly labyrinth area, fetal vessels seem to be expanded and trophoblast cell densities were lower in PE placenta compare to HP placenta (Figure 3.2C-D).

The total area of placenta from PE were significantly decreased from those of HP (Figure 3.2E). The area of junctional zone (JZ) layer to the total placenta major layers area in PE group were around 30% smaller than those observed in HP (Figure 3.2F).

3.4.3. Dynamics of the exosomes in the serum of healthy pregnancy and preeclampsia

In the mice serum of HP and PE, both EVs and exosomes were present in terms of total concentration and size (Table 3.1). Although the concentration of EVs showed no significant difference among groups, there was a significant reduction in their diameter. Additionally, while there was no change in exosome concentration, video drop analyses indicated that the percentage of exosomes in EVs in the PE group was higher compared to the HP group (Figure 3.3A). Exosome concentration was found to be higher in PE compared to HP, with values of 15.10 ± 2.93 (x10^8/mL) and 3.84 ± 1.01 (x10^8/mL) respectively.

TEM images revealed the round shape of vesicles ranging from 30-150 nm (Figure 3.3B). Furthermore, both the EVs marker (CD63) and specific-trophoblast marker (Syncytin) showed positive expression in all samples (Figure 3.3C), indicating that the isolated samples contained exosomes derived from placentas.

Table 3.3. Measurements of extracellular vesicles (EVs) and exosomes in the mouse serums

	Healthy pregnancy	Preeclampsia
Concentration of total EVs in serum ($x10^9$/mL)	4.05 ± 0.35	4.403 ± 1.10
Average EVs diameter in serum (nm)	242.83 ± 25.54[a]	191.33±5.48[a]
Rate of exosome-sized vesicles in total EVs (%)	9.46 ± 2.37[b]	34.76 ± 5.11[b]
Calculated concentration of exosomes in serum ($x10^8$/mL)	3.84 ± 1.01[c]	15.10 ± 2.93[c]
Average exosome diameter in EVs (nm)	128.86 ± 4.12	121.76 ± 1.21

[a-c] Significant differences were found between the same alphabet. Unpaired *t* test was applied. [a]$P<0.05$; [b,c]$P<0.01$

3.4.4. VEGF and iNOS protein expression after L-NAME administration

Immunohistochemistry showed weak to strong multifocal staining in all serial sections of the mouse placenta. Particularly, I found cells in the labyrinth area that reacted to the anti-VEGF and anti-iNOS antibodies (Figure 3.4-A). I noticed distinct differences in staining between HP and PE group in syncytiotrophoblast (STs) cells and the sinusoidal trophoblast cells (S-TCs) that are forming maternal blood sinuses. In HP placenta, there was weak positivity staining for VEGF in the STs and some cytoplasm of S-TCs, while staining was negative in the endothelial cells of fetal vessels. However, in cases of pre-eclampsia, I observed very intense and diffuse staining against anti-VEGF in all areas of the labyrinth, especially on the surface of the S-TCs and in the cytoplasm of some of these cells. Weak positive staining was also seen in STs. The staining patterns of iNOS were similar to VEGF, but stronger positivity was observed in PE placenta. Immuno-reactive score showed a moderate expression of VEGF and iNOS, significant higher in the PE group ($P<0.05$ and $P<0.01$), respectively (Figure 3.4B-C).

Western blot results of VEGF and iNOS in mouse serum-derived EVs were similar to the IHC results. A statistically significant increase was found for the PE group (Figure 3.4D).

3.4.5. Detection of miRNA in mouse serum-derived EVs

Real-time PCR study showed down-regulation of miR 16-3p and up-regulation of miR 25b-3p in the serum of pregnant mice with PE (Figure 3.5).

3.5. Discussion

I generated PE mouse model by administering L-NAME, which resulted in an increase in maternal systolic and diastolic BP above 140 and 90 mmHg, respectively. Along with hypertension, our PE mice also exhibited proteinuria and fetal growth restriction (FGR). In other hand, the placentas of PE mice had lower weights compared to HP. These findings are in similar with previous studies (Motta et al., 2015; Yoshikawa et al., 2017).

Histopathological investigation revealed expanded the fetal vessels and reduced the number of S-TGCs in the labyrinth area. Vasodilation in fetal vessels occurs as a mechanism to enhance blood flow to the fetus, which in this case lacks oxygen and/or nutrients (Ramanlal and Gupta, 2023). S-TGCs are crucial for maintaining the structure of maternal circulation within labyrinth (Soncin *et al.,* 2015). They form cytoplasmic bridges that connect across maternal blood spaces and contribute to the development of maternal sinusoids (Coan *et al.,* 2005; Outhwaite *et al.,* 2015). A decrease in the number of S-TGCs may impair labyrinth vascular elaboration, leading to a reduced surface area for exchange (Outhwaite *et al.,* 2015). Moreover, S-TGCs facilitate the transport of secreted factors like hormones (Simmons et al., 2008; Coan *et al.,* 2005). The reduction of S-TGCs removes critical endocrine signals, the absence of which adversely affects fetal growth (Outhwaite *et al.,* 2015). These results demonstrate that fetal development is closely linked to placental formation, and L-NAME has a negative impact on placentation that leads to FGR. Meanwhile, decreasing in the ratio of JZ to total placenta area suggest that L-NAME-induced PE were probably caused by placental cellular damage, which might affect maternal-fetal exchange.

I demonstrated that VEGF expression was higher not only in the placenta tissue affected by PE but also in PE serum-derived EVs. These findings are in accord with the observations of Kurbanov *et al.* (2018) and Hunter *et al.* (2000) who proposed VEGF as a marker of PE. It is known that placentation involves extensive angiogenesis to establish a proper vascular

network between the mother and fetus (Ferris, 1991; Runyan *et al.,* 2019; Roberts *et al.,* 1989). However, while VEGF is important for vasculogenesis and angiogenesis, increasing VEGF expression at least two times can disrupt embryo development (Miquerol *et al.,* 2000). Additionally, sFlt1, an angiogenic inhibitor is known to be elevated in PE (Cohen *et al.,* 2015). In a mouse study reported by Jena *et al.* (2000), it was found that increased of VEGF in the endometrium leads to increased placental sFlt-1, resulting PE-like symptoms in the mother, damage to placental vasculature, and fetal death. This indicates that restricting VEGF levels is crucial for placental development and fetal survival. Furthermore, an exogenous VEGF could induce PE-like symptoms in pregnant mice, indicating that VEGF plays a major role in the pathophysiology of PE (Murakami *et al.,* 2005).

Using IHC and WB, upregulation of iNOS in our results is consistent with the findings of Miller et al. (1996) and Du et al. (2017). iNOS is known to be stimulated in proinflammatory or inflammatory conditions, leading to a temporary excess of nitric oxide (NO). Since PE is associated with increased inflammation (Du et al., 2017), this finding is significant. Additionally, endoplasmic reticulum (ER) stress has also been reported in PE, which mediates the induction of reactive oxygen species (ROS) and NO. The Ire1 protein, a type of ER stress-related marker, was elevated in PE, which may activate proinflammatory pathways and induce iNOS upregulation (Du et al, 2017). In the other hand, L-NAME works by inhibiting NOS, the enzymes for producing NO (Pfeiffer *et al.,* 1996). However, the self-regulating properties of NO have a dual effect only in the expression of iNOS (Azizi et al., 2019). At low concentrations, NO acts as positive feedback, upregulate iNOS. As negative feedback, high concentration NO reduces the iNOS activity. Furthermore, L-NAME was shown to increase the transcription of the iNOS gene (Weisz et al., 1996; Miller et al., 1996), suggesting that NO interferes with iNOS expression. Miller et al. (1996) reported that the induction of iNOS expression to normalize NO production should be considered as an additional regulatory

response in a state of NO shortage. They concluded that iNOS expression is responsible for a compensatory increase or normalization of NO synthesis during sustained administration of L-NAME.

Here, we demonstrated that PE exosomes increase as compared to HP, which consistent with previous reports (Salomon, 2017; Pillay et al., 2016). PE is known not only associated with changes in the circulating levels of exosomes, but also in their miRNA content. In this study, two out of four miRNAs showed different dynamics from those in PE mouse serum-derived EVs. There is a possibility that miR 16-5p and miR 25b-3p are dysregulated and play a role in the pathogenesis of PE.

Several studies reported that miR-16 can significantly inhibit cell proliferation and invasion, promote cell apoptosis, and suppress cell cycle progression. It also reduces inflammation by suppressing pro-inflammatory factors (Rivas *et al.,* 2012; Wang *et al.,* 2012). MiR-16 is known to regulate placental angiogenesis by directly modulating the expression of VEGF (Zhu *et al.,* 2016; Chamorro-Jorganes *et al.,* 2011; Witvrouwen *et al.,* 2021). Furthermore, overexpressed exomiR-16 is negatively correlated with the levels of VEGFA that influences proliferation and migration of trophoblasts and angiogenesis processes (Wang *et al.,* 2012). It suggests that low expression of miR-16 may induce inflammation and increase the protein level of VEGF, potentially contributing to the development of PE.

On the other hand, the expression of miR-25-3p was found to increase along with systolic and diastolic blood pressure and urine protein levels in PE (Zhou *et al.,* 2022). Additionally, exomiR-25b-3p transmitted by the trophoblasts under inflammatory conditions has been implicated in fetal growth restriction (Wang *et al.,* 2021). This suggests that high expression of miR-25-3p is linked to a higher risk of adverse pregnancy outcomes.

In conclusion, exosomes in PE may contain miRNAs that exhibit characteristics of injured trophoblasts. Therefore, analyzing exomiRs could help in predicting the onset of PE.

Additionally, exomiRs could be potential targets for treating PE. Since exomiRs can contribute to the occurrence and progression of PE through various pathways, inhibiting their expression and blocking these pathways may be effective in treating PE.

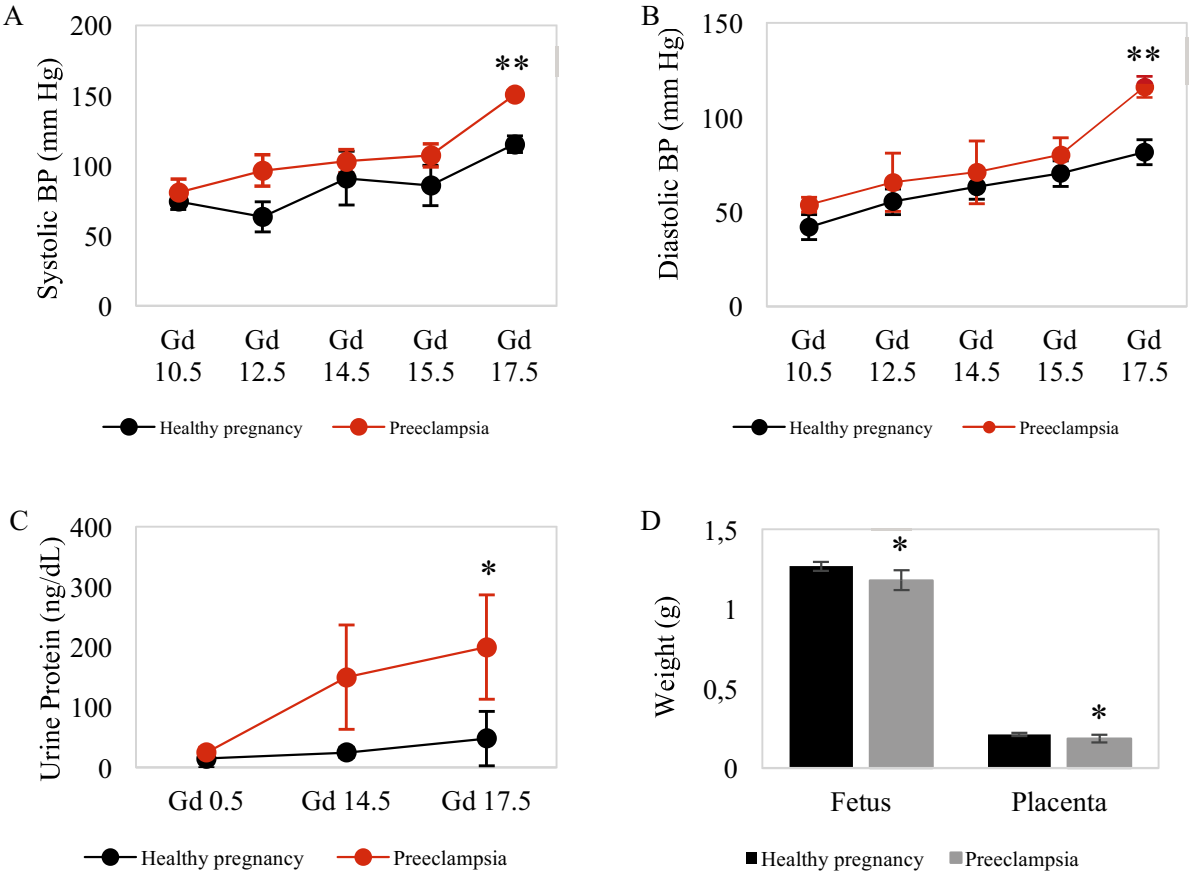

E Healthy pregnancy

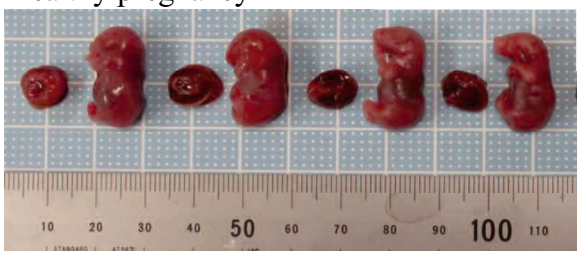

Preeclampsia

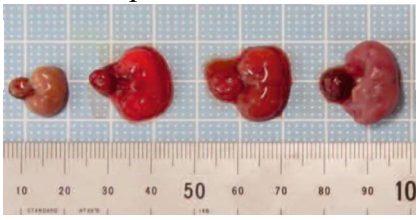

Figure 3.1. Preeclampsia phenotype were observed in the L-NAME-induced PE mouse model. Changes in systolic blood pressure (A), diastolic blood pressure (B), and urinary protein concentration during pregnancy (C). Fetus and placenta weight at gestational day (Gd) 17.5 (D). Macroscopic appearance of fetus and placenta at Gd 17.5 (E). *P<0.05, **P<0.01.

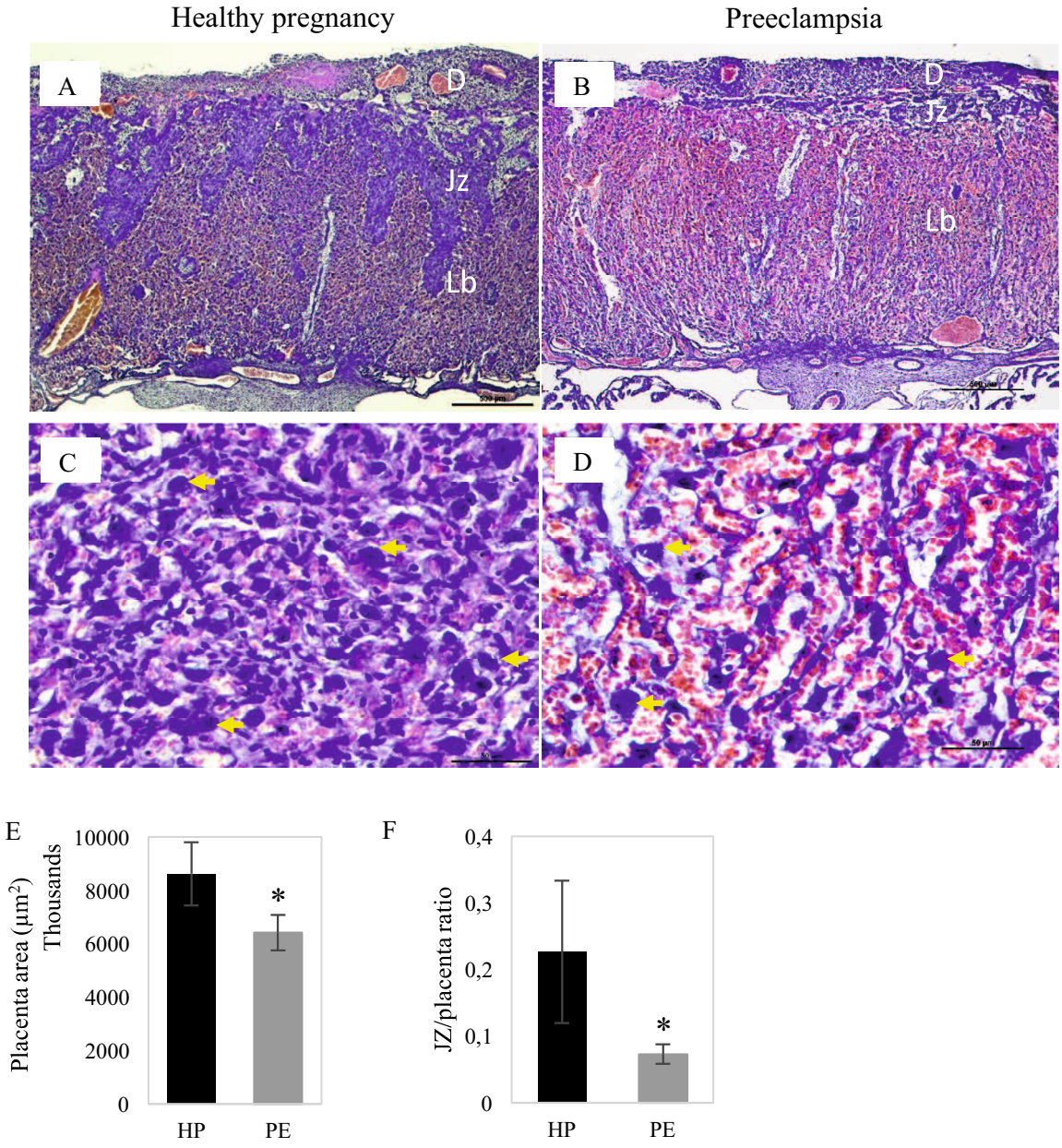

Figure 3.2. Histopathological examination of placenta. Pregnant mice were treated subcutaneously with L-NAME 50 mg/kgBW/day (PE) or PBS (HP) from Gd 7.5 to Gd 17.5. At Gd 17.5, section of placenta from PBS (A, C) or L-NAME induced preeclampsia mice (B, D) were stained with Haematoxylin and Eosin (HE). Image C and D are enlarged images of the labyrinth area within the rectangle box in A and B, respectively. The area of the placenta (E) and the ratio of junctional zone area to the total placenta area (F) were assessed by examining the HE-stained section in A and B and were analysed quantitatively. *P<0.05 by t-test. HP=healthy pregnancy; PE=preeclampsia; D=decidua; Jz=junctional zone; Lb=labyrinth. Yellow arrow indicates sinusoid trophoblast giant cells (S-TCs).

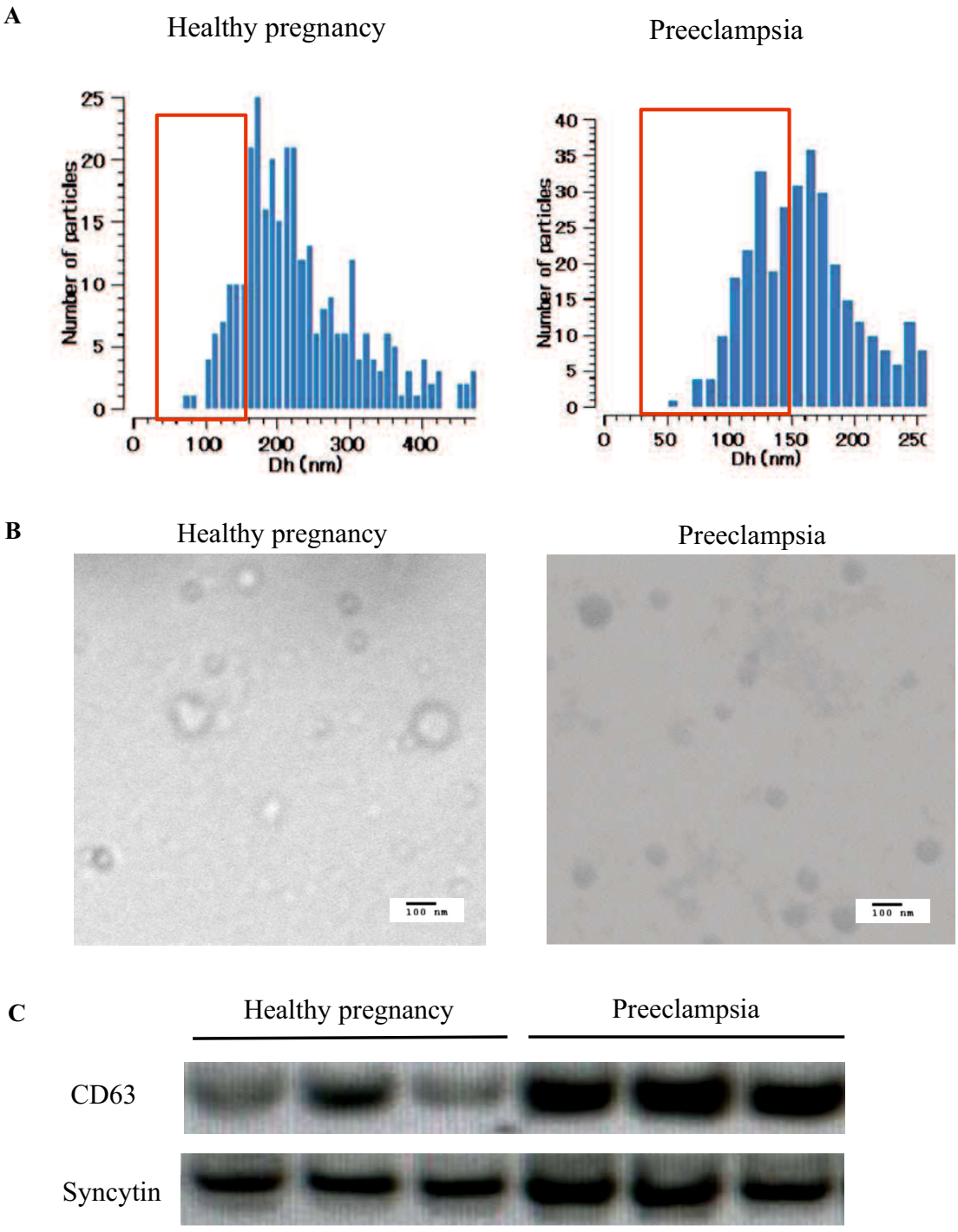

Figure 3.3. Characterization of extracellular vesicles (EVs). EVs isolated from mouse pregnant serum was confirmed using video drop (A), transmission electron microscope (TEM) (B), and western blot (C).

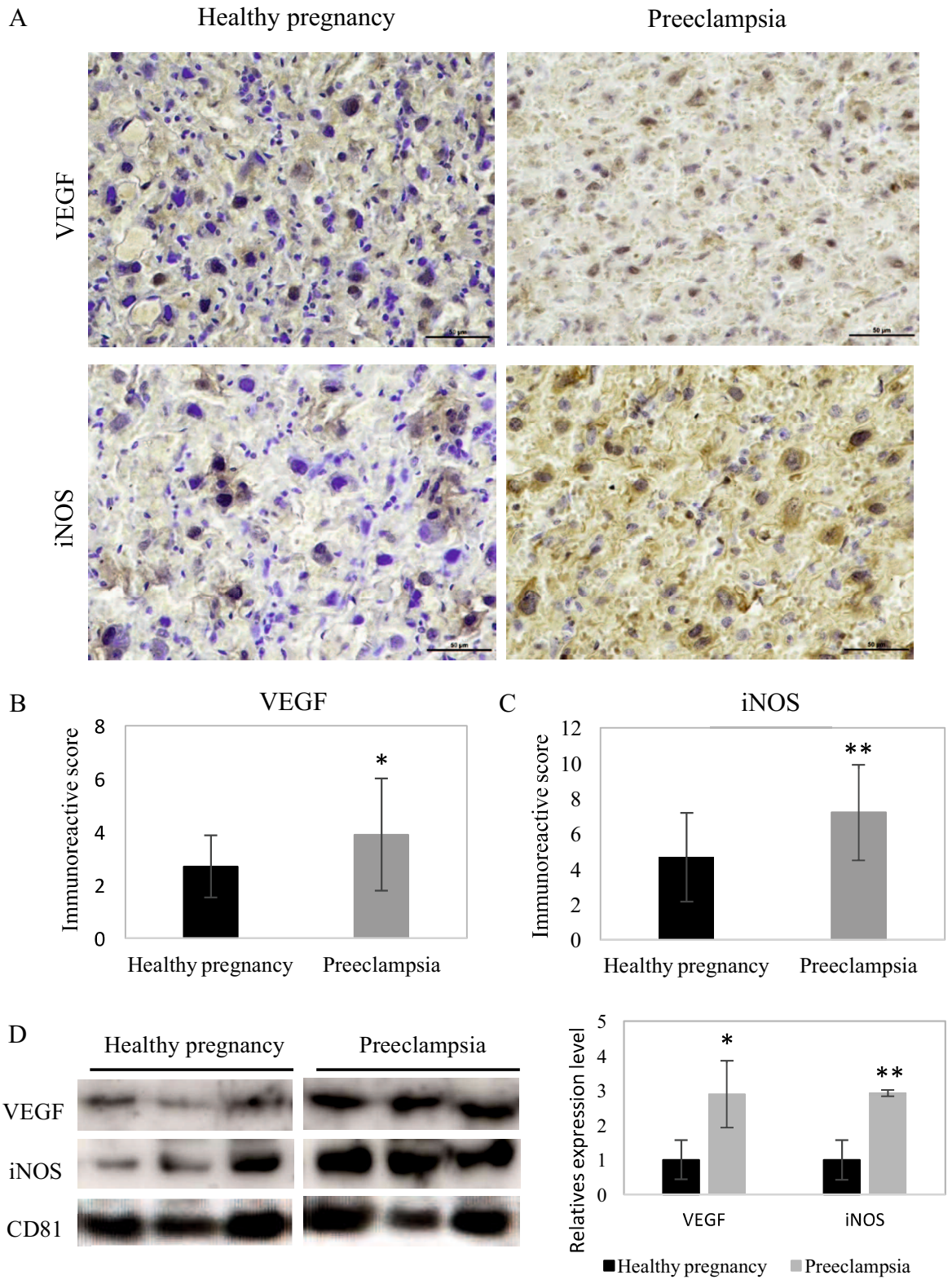

Figure 3.4. Immunohistochemical staining and western blot analyses of VEGF and iNOS in placental tissues and serum-derived EVs from healthy pregnancy mouse and those with PE. Representative immunostaining of iNOS and VEGF (brown) in placenta tissue (A). Immunoreactive score of VEGF (B) and iNOS (C). Western blot analyses of VEGF and iNOS in serum-derived EVs (D). **P*<0.05; ***P*<0.01

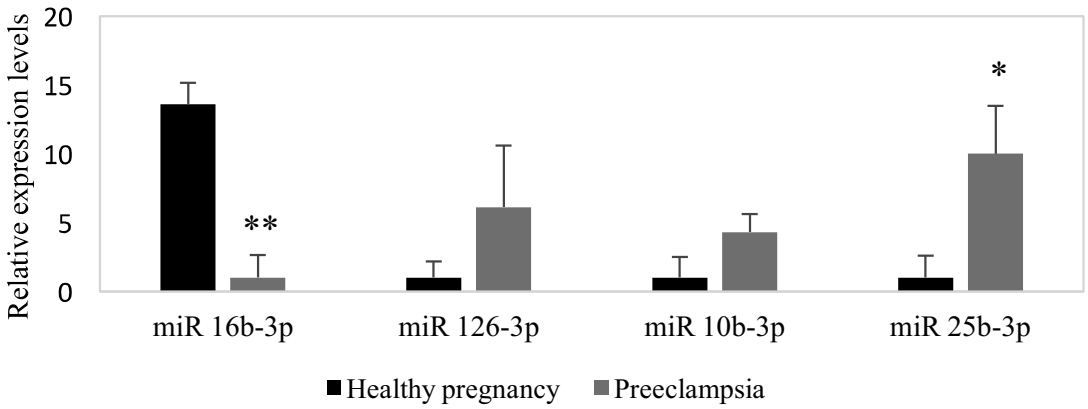

Figure 3.5. miRNAs in the serum-derived EVs were detected by qPCR. Quantification results are displayed relative to the lower amount of each miRNA as 1.0. *P<0.05, **P<0.01.

GENERAL DISCUSSION AND CONCLUSION

Pregnancy is an immunological phenomenon in which the mother can tolerate the semi-allogenic fetus for a defined period through tightly regulated biological processes. Although the exact mechanisms involved in this process have not been fully understood, the main mechanism is the ability of the placental syncytiotrophoblast cells to promote immune tolerance and regulate migration and invasion into the maternal decidua. While the specific cellular molecular mechanisms in pregnancy are not completely understood, exosomes have been identified as a key component of the placental microenvironment. They play a crucial role in initiating and maintaining multi-layered cellular communication directed towards trophoblast invasion during placental development. Moreover, the placenta has been shown to release exosomes (termed placental-derived exosomes) which are key factors in the immunomodulation of pregnancy and its related complications. This has been mainly attributed to their physiological role in regulating feto–maternal immune tolerance and the maternal metabolic adaptation to gestation.

Exosomes, which are tiny vesicles ranging from 30 to 150 nanometers in size and derived from multivesicular bodies, contain nucleic acids, proteins, and lipids. They have been shown to promote physiological functions through various signaling mechanisms such as autocrine, paracrine, and endocrine pathways. Exosomes can bind to target cells or organs, reprogramming them through direct signaling via surface proteins or by delivering their cargo inside the cells. In disease states, this property allows these vesicles to directly mediate end-organ damage, making them promising candidates as biomarkers for early disease diagnosis and prognosis. Recently, exosomal microRNAs (exomiR) have emerged as important biomarkers for several disease states, as they are selectively packaged into exosomes and released by the cells to participate in cellular reprogramming. Some studies have highlighted

the crucial role of micro RNAs (miRNAs) in regulating normal placental development and the pathogenesis of preeclampsia, leading to a better understanding of exomiR. My studies provide essential insights into the role of exosomes in normal pathophysiology and the development of preeclampsia (PE).

In my initial chapter, I focused on the analysis of pregnant canine serum and its variations during gestation. I identified three genes that are specifically expressed in the canine placenta: RLN2, LCN2, and TFPI2. During normal pregnancy, increased levels of RLN2 protein in the serum are believed to be involved in angiogenesis regulation, while elevated levels of LCN2 protein are thought to be necessary for trophoblast invasion. Additionally, increased levels of TFPI2 protein are associated with blood coagulation in the canine placenta. I also observed the presence of exosomes in all pregnant canine serums, although they accounted for less than 6% of the total extracellular vesicles (EVs). Histological examination revealed a large number of secretory vesicles at the spongy layer, which were predominantly large in size, indicating that microvesicles or cell debris dominated over exosomes. This suggests that exosomes produced in fetal tissue may have difficulty reaching maternal blood due to the canine placenta's endotheliochorial type and thick-layered fetomaternal boundary compared to the hemochorial type in mice (evidence shows an increase in exosomes during gestational periods in mice). Furthermore, my findings indicated the presence of cell-free RNA related to RLN2 in maternal canine serum above a certain threshold did not correlate with changes in canine exosome concentrations during gestation, suggesting that RLN2 does not significantly increase. However, successful detection of RLN2 suggests the possibility of specific marker genes for cell-free RNA. Although their role may be smaller than in mice, factors encompassed in exosomes may still be present and reflect fetal development and placental formation in pregnant dog serum. In conclusion, I successfully identified specific genes in the canine placenta and tracked the transition of their translated proteins into the blood.

These placenta-derived genes can serve as an effective tool for monitoring maternal endocrine conditions, fetal growth, and successful pregnancy progression. These findings are valuable for understanding the physiology of canine pregnancy and have potential applications in clinical reproduction.

In the second chapter of my study, I conducted experiments using mice. I demonstrated the changes in EVs and exosomes in the circulating blood of pregnant mice. I interested to identify a tetraspanin marker that consistently appeared with exosomes. I found that the percentage of mouse exosomes detected by nanoparticle-tracking assay (NTA) in EVs was 53% at NP and significantly increased to almost 100% at Gd 18.5 in normal pregnancy. The concentration of exosomes was significantly higher from Gd 10.5 and reached its maximum just before parturition. Among the tetraspanin markers used to characterize EVs, the CD63 antibody was found to be the most consistent with exosome appearance detected by NTA. Furthermore, serum exosomes showed a positive reaction to the syncytiotrophoblast marker, syncytin-1, indicating that some exosomes isolated from pregnant serum were derived from the placenta. Immunohistochemistry using anti-CD63 antibody showed positive reactions in mouse placentas at the syncytiotrophoblasts and endothelial cells of the fetal capillaries, representing the first report of exosome localization in the mouse placenta tissue. These findings indicated that the CD63 tetraspanin marker is useful in identifying the dynamics and localization of mouse exosomes. ExomiRs detection by RT-qPCR showed significantly higher amounts of exomiR-10b-3p, exomiR-25b-3p, and exomiR-143-3p in the exosomes of Gd 18.5. MiR-10b-3p is found in the PE mouse model and affects the viability, migration, and invasion of trophoblasts. MiR-25b-3p is suggested to be associated with adverse pregnancy outcomes including hypertensive disorders, fetal growth restriction, and preterm birth. Under normal pregnancy, placentas can transport miR-25-3p to the myometrium to maintain calcium homeostasis and contribute to avoiding preterm birth. Meanwhile, miR-143-3p is essential for

successful embryo implantation in mice. Studies in humans revealed that miR-143-3p regulates adipogenic growth in pregnancy to prevent excessive fetal growth. More interestingly, there was a size reduction of exosomes at Gd 18.5. Mouse exosomes were predominantly Exo-L (90-120 nm) at non-pregnant, Gd 6.5, 10.5, and 14.5, and then converted to Exo-S (60-80 nm) at Gd 18.5. The proteome analyses showed that the cargo proteins in Exo-L were rich in those involved in IL-2/STAT5 signaling and the immunomodulation pathway, which is associated with an increase of regulatory T (Treg) cells during early pregnancy. Treg cells suppress maternal allogeneic responses directed against the fetus, and their depletion leads to pregnancy failure. Particularly during implantation and early placentation, the Treg effect by Exo-L may be necessary for the establishment of pregnancy. These findings suggest that exosomes are produced in the mouse placenta and transferred to maternal or fetal bloodstreams, which is expected to have a miRNA-mediated physiological effect and become useful biomarkers reflecting the pregnancy status. In summary, my findings show that mouse serum EVs are mainly composed of exosomes derived from completed placentas. Several miRNAs encapsulated in exosomes were present in maternal serum at Gd 18.5 and are involved in the mice physiology of normal pregnancy. These results will be useful in studying the normal pregnancy process, analyzing pathological human models of abnormal pregnancy, and developing monitoring molecules for pregnancy complications.

My third chapter discussed the role of exosomes and their variations of physiological factors and miRNAs in a PE mouse model injected by L-NAME. In this study, I found that although no change in the total concentration of EVs, exosomes released more abundantly in the serum of the PE mouse model compared to healthy pregnancies. In PE, vessel endothelial growth factor (VEGF) concentrations have been measured in the maternal circulation by different investigators compared to normal pregnancies with conflicting results including increases, decreases, and no change. The discrepancies may reflect study design as well as the

use of a variety of assays that may not always be reliable in pregnancy. In this study, I found that VEGF expression is higher not only in the placenta tissue affected by PE but also in PE serum-derived EVs. While VEGF is important for vasculogenesis and angiogenesis, increasing VEGF expression at least two times can disrupt embryo development. In a mouse study, it was reported that increased VEGF in the endometrium leads to increased placental sFlt-1 (an angiogenic inhibitor that is known to be elevated in PE), resulting in PE-like symptoms in the mother, damage to placental vasculature, and fetal death. This indicates that restricting VEGF levels is crucial for placental development and fetal survival. Additionally, an exogenous VEGF could induce PE-like symptoms in pregnant mice, indicating that VEGF plays a major role in the pathophysiology of PE. On the other hand, L-NAME that are used to exhibit PE in this study works by inhibiting nitric oxide synthetase (NOS), the enzymes for producing nitric oxide (NO). More interestingly, iNOS was found to be upregulated in both placenta tissue and serum-derived EVs. The self-regulating properties of NO are known to have a dual effect on the expression of NOS. It means that low concentrations of NO act as positive feedback and upregulate iNOS, while as negative feedback, high concentration NO reduces the iNOS activity. The induction of iNOS expression occurs to normalize NO production in a state of NO shortage as a regulatory response. iNOS is also stimulated in proinflammatory or inflammatory conditions, leading to a temporary excess of nitric oxide (NO). Since PE is associated with increased inflammation, my finding is significant. Regarding the elevation of exosomes concentration in PE mice, I found upregulation of exomiR-25b-3p and downregulation of exomiR 16-5p, which is possible to play a role in the pathogenesis of PE. The expression of miR-25-3p was found to increase along with systolic and diastolic blood pressure and urine protein levels in PE. ExomiR-25b-3p transmitted by the trophoblasts under inflammatory conditions has been implicated in fetal growth restriction. Meanwhile, miR-16 can significantly reduce inflammation by suppressing pro-inflammatory factors. Interestingly,

miR-16 is known to regulate placental angiogenesis by directly modulating the expression of VEGF. Overexpressed exomiR-16 is known to have a negative correlation with the levels of VEGF, which influences the proliferation and migration of trophoblasts and angiogenesis processes. It is suggested that low expression of miR-16 may induce inflammation and increase the protein level of VEGF, potentially contributing to the development of PE. In conclusion, exosomes in PE may contain miRNAs that exhibit characteristics of injured trophoblasts. Therefore, analyzing exomiRs could help in predicting the onset of PE. Additionally, exomiRs could be potential targets for treating PE. Since exomiRs can contribute to the occurrence and progression of PE through various pathways, inhibiting their expression and blocking these pathways may be effective in treating PE.

Taken together, this dissertation reported that exosomes in maternal circulation contain microRNAs which are linked to biological pathways both in normal pregnancy and pregnancy disorder, particularly preeclampsia. Total exosome concentration in the serum of a pregnant mother may be affected by placental types in mammals as there are no changes in canines and horses (unpublished data). However, the miRNA profile possibly changes during the pregnancy progression and involved in the pathophysiology of pregnancy. Furthermore, the pathogenesis of PE has not been fully elucidated, and its early diagnosis, prevention, and treatment are significant but currently limited. Synthesis of exosomes containing miRNAs is influenced by various factors such as hypoxia and they may contribute to the significant changes in protein expression observed in PE, resulting in dysfunction in both maternal and maternal-fetal circulation and subsequent impairment of angiogenesis, which is the key feature of PE. The ability to identify exosomal miRNA generated during pregnancy and implement non-invasive therapies to mitigate their effects may prove critical in clinical applications for the diagnosis, prediction, and treatment of PE. For example, it may be helpful for the diagnosis and prediction of PE by detecting the expression levels of exosomal miRNA and transcripts.

Additionally, targeting exosomal miRNAs and related pathways may have great potential for the treatment of PE. However, further research is warranted to identify the mechanisms underlying the release of exosomal miRNAs involved in PE progression.

I believe this research would be interesting for all readers who are interested in the physiological reproduction of mammals during pregnancy associated with extracellular vesicle communications.

REFERENCES

Abdel-Rahman RF, Hessin AF, Abdelbaset M, Ogaly HA, Abd-Elsalam RM, Hassan SM. 2017. Antihypertensive effects of roselle-olive combination in L-NAME-induced hypertensive rats. *Oxid Med Cell Longev* **2017**: 9460653.

Ali MN, Kasetty G, Elvén M, Alyafei S, Jovic S, Egesten A, Herwald H, Schmidtchen A, Papareddy P. 2018. TFPI-2 protects against gram-negative bacterial infection. *Front Immunol* **9**: 2072.

Aluvihare VR, Kallikourdis M, Betz AG. 2004. Regulatory T cells mediate maternal tolerance to the fetus. *Nat Immunol* **5**: 266–271.

Asai H, Ikezu S, Tsunoda S, Medalla M, Luebke J, Haydar T, Wolozin B, Butovsky O, Kügler S, Ikezu T. 2015. Depletion of microglia and inhibition of exosome synthesis halt tau propagation. *Nat Neurosci* **18**(11): 1584-93.

Azizi M, Moradi M, Johari B, Rafiee, MH. 2019. Simultaneous comparison of L-NAME and melatonin effects on RAW 264.7 cell line's iNOS production and activity. *Turkish J of Biochemistry* **44**(6): 840-847.

Bai K, Li X, Zhong J, Ng EHY, Yeung WSB, Lee CL, Chiu PCN. 2021. Placenta-derived exosomes as a modulator in maternal immune tolerance during pregnancy. *Front Immunol* **12**: 671093.

Bang C, Thum T. 2012. Exosomes: new players in cell-cell communication. *Int J Biochem Cell Biol* **44**: 2060–2064.

Bates DO. 2010. Vascular endothelial growth factors and vascular permeability. *Cardiovasc Res* **87**(2): 262-71.

Borges F, Reis L, Schor N. 2013. Extracellular vesicles: Structure, function, and potential clinical uses in renal diseases. *Braz J Med Biol Res* **46**: 824–830.

Brosens IA, Robertson WB, Dixon HG. 1972. The role of the spiral arteries in the pathogenesis of preeclampsia. *Obstet Gynecol Annu* **1**: 177–191.

Burton GJ, Woods AW, Jauniaux E, Kingdom JCP. 2009. Rheological and physiological consequences of conversion of the maternal spiral arteries for uteroplacental blood flow during human pregnancy. *Placenta* **30**: 473–482.

Cebova M, Klimentova J, Janega P, Pechanova O. Effect of bioactive compound of Aronia melanocarpa on cardiovascular system in experimental hypertension. 2017. *Oxid Med Cell Longev* **2017**: 8156594.

Cesur S, Yucel A, Noyan V, Sagsoz N. 2012. Plasma lipocalin-2 levels in pregnancy. *Acta Obstet Gynecol Scand* **91**: 112–116.

Chamorro-Jorganes A, Araldi E, Penalva LO, Sandhu D, Fernández-Hernando C, Suárez Y. 2011. MicroRNA-16 and microRNA-424 regulate cell-autonomous angiogenic functions in endothelial cells via targeting vascular endothelial growth factor receptor-2 and fibroblast growth factor receptor-1. *Arterioscler Thromb Vasc Biol* **31**: 2595–2606

Chen L, Hou J, Ye L, Chen Y, Cui J, Tian W, Li C, Liu L. 2014. MicroRNA-143 regulates adipogenesis by modulating the MAP2K5-ERK5 signaling. *Sci Rep* **4**: 3819.

Cheng L, Sharples RA, Scicluna BJ, Hill AF. 2014. Exosomes provide a protective and enriched source of miRNA for biomarker profiling compared to intracellular and cell-free blood. *J Extracell Vesicles* **3**: 23743.

Chernyshev VS, Rachamadugu R, Tseng YH, Belnap DM, Jia Y, Branch KJ, Butterfield AE, Pease LF 3rd, Bernard PS, Skliar M. 2015. Size and shape characterization of hydrated and desiccated exosomes. *Anal Bioanal Chem* **407**: 3285–3301.

Coan PM, Ferguson-Smith AC, Burton GJ. 2005. Ultrastructural changes in the interhaemal membrane and junctional zone of the murine chorioallantoic placenta across gestation. *J Anat* **207**: 783-796.

Cohen JM, Kramer MS, Platt RW, Basso O, Evans RW, Kahn SR. 2015. The association between maternal antioxidant levels in midpregnancy and preeclampsia. *Am J Obstet Gynecol* **213**:695.

Cohen M, Meisser A, Bischof P. 2006. Metalloproteinases and human placental invasiveness. *Placenta* **27**: 783–793.

Colombo M, Raposo G, Théry C. 2014. Biogenesis, secretion, and intercellular interactions of exosomes and other extracellular vesicles. *Annu Rev Cell Dev Biol* **30**: 255–289.

Concannon PW, McCann JP, Temple M. 1989. Biology and endocrinology of ovulation, pregnancy and parturition in the dog. *J Reprod Fertil Suppl* **39**: 3–25.

Condrat CE, Varlas VN, Duică F, Antoniadis P, Danila CA, Cretoiu D, et al. 2021. Pregnancy-related extracellular vesicles revisited. *Int J Mol Sci* **2**(8): 3904.

Cronqvist T, Tannetta D, Mörgelin M, Belting M, Sargent I, Familari M, Hansson SR. 2017. Syncytiotrophoblast derived extracellular vesicles transfer functional placental miRNAs to primary human endothelial cells. *Sci Rep* **7**: 4558.

Czernek L, Düchler M. 2020. Exosomes as messengers between mother and fetus in pregnancy. *Int J Mol Sci* **21**: 4264.

de Alwis N, Binder NK, Beard S, Mangwiro YT, Kadife E, Cuffe JS, Keenan E, Fato BR, Kaitu'u-Lino TJ, Brownfoot FC, Marshall SA, Hannan NJ. 2022. The L-NAME mouse model of preeclampsia and impact to long-term maternal cardiovascular health. *Life Sci Alliance* **5**(12): e202201517.

de Jong OG, Verhaar MC, Chen Y, Vader P, Gremmels H, Posthuma G, Schiffelers RM, Gucek M, van Balkom BWM. 2012. Cellular stress conditions are reflected in the protein and RNA content of endothelial cell-derived exosomes. *J Extracell Vesicles* **1**: 18396.

Ding Y, Hu Q, Gan J, Zang X, Gu T, Wu Z, Cai G, Hong L. 2022. Effect of miR-143-3p from extracellular vesicles of porcine uterine luminal fluid on porcine trophoblast cells. *Animals (Basel)* **12**: 3402.

Diomaiuto E, Principe V, De Luca A, Laperuta F, Alterisio C, Di Loria A. 2021. Exosomes in dogs and cats: An innovative approach to neoplastic and non-neoplastic diseases. *Pharmaceuticals (Basel)* **14**(8): 766.

Du, L., He, F., Kuang, L. *et al.* 2017. eNOS/iNOS and endoplasmic reticulum stress-induced apoptosis in the placentas of patients with preeclampsia. *J Hum Hypertens* **31**: 49–55.

Fader CM, Sánchez D, Furlán M, Colombo MI. 2008. Induction of autophagy promotes fusion of multivesicular bodies with autophagic vacuoles in k562 cells. *Traffic* **9**: 230–50.

Fainboim L, Arruvito L. 2011. Mechanisms involved in the expansion of Tregs during pregnancy: role of IL-2/STAT5 signaling. *J Reprod Immunol* **88**: 93–98.

Ferraresso S, Bresolin S, Aricò A, Comazzi S, Gelain ME, Riondato F, Bargelloni L, Marconato L, Kronnie G, Aresu L. 2014. Epigenetic silencing of TFPI-2 in canine diffuse large B-cell lymphoma. PLoS One 9: e92707.

Ferris TF. 1991. Pregnancy, preeclampsia, and the endothelial cell. *N Engl J Med* **325**: 1439–1440.

Geddings JE, Mackman N. 2013. Tumor-derived tissue factor-positive microparticles and venous thrombosis in cancer patients. Blood 122: 18731880.

Ghafourian M, Mahdavi R, Akbari Jonoush Z et al. 2022. The implications of exosomes in pregnancy: emerging as new diagnostic markers and therapeutics targets. *Cell Commun Signal* **20**: 51.

Gill M, Motta-Mejia C, Kandzija N, Cooke W, Zhang W, Cerdeira AS, Bastie C, Redman C, Vatish M. 2019. Placental syncytiotrophoblast-derived extracellular vesicles carry active nep (neprilysin) and are increased in preeclampsia. *Hypertension* **73**(5): 1112-1119.

Guo XR, Ma Y, Ma ZM, Dai TS, Wei SH, Chu YK, Dan XG. 2023. Exosomes: The role in mammalian reproductive regulation and pregnancy-related diseases. *Front Physiol* **10**(14): 1056905.

Hessvik NP, Llorente A. 2018. Current knowledge on exosome biogenesis and release. *Cell Mol Life Sci* **75**: 193–208.

Heusermann W, Hean J, Trojer D, Steib E, von Bueren S, Graff-Meyer A, Genoud C, Martin K, Pizzato N, Voshol J, Morrissey DV, Andaloussi SE, Wood MJ, Meisner-Kober NC. 2016. Exosomes surf on filopodia to enter cells at endocytic hot spots, traffic within endosomes, and are targeted to the ER. *J Cell Biol* **213**: 173–184.

Hoffmann B, Höveler R, Nohr B, Hasan SH. 1994. Investigations on hormonal changes around parturition in the dog and the occurrence of pregnancyspecific non-conjugated oestrogens. *Exp Clin Endocrinol* **102**: 185–189.

Hood JD, Meininger CJ, Ziche M, et al. 1998. VEGF upregulates ecNOS message, protein, and NO production in human endothelial cells. *Am J Physiol* **274**(3 Pt 2): H1054–H1058.

Hoover-Plow J. 2010. Does plasmin have anticoagulant activity? *Vasc Health Risk Manag* **6**: 199–205.

Hoshino A, Costa-Silva B, Shen TL, Rodrigues G, Hashimoto A, Tesic Mark M, Molina H, Kohsaka S, Di Giannatale A, Ceder S, Singh S, Williams C, Soplop N, Uryu K, Pharmer L, King T, Bojmar L, Davies AE, Ararso Y, Zhang T, Zhang H, Hernandez J, Weiss JM, Dumont-Cole VD, Kramer K, Wexler LH, Narendran A, Schwartz GK, Healey JH, Sandstrom P, Labori KJ, Kure EH, Grandgenett PM, Hollingsworth MA, de Sousa M, Kaur S, Jain M, Mallya K, Batra SK, Jarnagin WR, Brady MS, Fodstad O, Muller V, Pantel K, Minn AJ, Bissell MJ, Garcia BA, Kang Y, Rajasekhar VK, Ghajar CM, Matei I, Peinado H, Bromberg J, Lyden D. 2015. Tumour exosome integrins determine organotropic metastasis. *Nature* **527**(7578): 329-35.

Hou Z, Romero R, Uddin M, Than NG, Wildman DE. 2009. Adaptive history of single copy genes highly expressed in the term human placenta. *Genomics* **93**: 33–41.

Hunter A, Aitkenhead M, Caldwell C, McCracken G, Wilson D, McClure N. 2000. Serum levels of vascular endothelial growth factor in preeclamptic and normotensive pregnancy. *Hypertension* **36**: 965–969.

James MR, August PA, Bakris G, Barton JR, Bernstein IM, Druzin M, Gaiser RR, Granger JR, Jeyabalan A, Johnson DD, Karumanchi SA, Lindheimer M, Owens MY, Saade GR, Sibai BM, Spong CY, Tsigas E, Joseph GF, O'Reilly N, Politzer A, Son S, Ngaiza K. 2013. Hypertension in pregnancy: executive summary. *Obstet Gynecol* **122**(5): 1122-1131.

Jena MK, Sharma NR, Petitt M, Maulik D, Nayak NR. 2020. Pathogenesis of preeclampsia and therapeutic approaches targeting the placenta. *Biomolecules* **10**(6): 953.

Ji L, Brkić J, Liu M, et al. 2013. Placental trophoblast cell differentiation: physiological regulation and pathological relevance to preeclampsia. *Mol Aspects Med* **234**(5): 981–1023.

Jin J, Menon R. 2018. Placental exosomes: A proxy to understand pregnancy complications. *Am J Reprod Immunol* **79**: e12788.

Karumanchi SA, Stillman IE, Lindheimer MD. 2009. Angiogenesis and preeclampsia. *Chesley's Hypertensive Disorders in Pregnancy*, 87–103.

Khan H, Kusakabe KT, Wakitani S, Hiyama M, Takeshita A, Kiso Y. 2012. Expression and localization of NO synthase isoenzymes (iNOS and eNOS) in development of the rabbit placenta, *J Reprod and Develop* **58**(2): 231-236.

Khushman M, Bhardwaj A, Patel GK, Laurini JA, Roveda K, Tan MC, Patton MC, Singh S, Taylor W, Singh AP. 2017. Exosomal markers (CD63 and CD9) expression pattern using Immunohistochemistry in resected malignant and nonmalignant pancreatic specimens. *Pancreas*. **46**: 782–788.

Kim DK, Kang B, Kim OY, Choi DS, Lee J, Kim SR, Go G, Yoon YJ, Kim JH, Jang SC, Park KS, Choi EJ, Kim KP, Desiderio DM, Kim YK, Lötvall J, Hwang D, Gho YS. 2013. EVpedia: an integrated database of high-throughput data for systemic analyses of extracellular vesicles. *J Extracell Vesicles* **2**: 20384.

Klohonatz KM, Cameron AD, Hergenreder JR, da Silveira JC, Belk AD, Veeramachaneni DN, Bouma GJ, Bruemmer JE. 2016. Circulating miRNAs as Potential Alternative Cell Signaling Associated with Maternal Recognition of Pregnancy in the Mare. *Biol Reprod* **95**(6): 124.

Kobara H, Miyamoto T, Suzuki A, Asaka R, Yamada Y, Ishikawa K, Kikuchi N, Ohira S, Shiozawa T. 2013. Lipocalin2 enhances the matrix metalloproteinase-9 activity and invasion of extravillous trophoblasts under hypoxia. *Placenta* **34**: 1036–1043.

Kowalewski MP, Tavares Pereira M, Kazemian A. 2020. Canine conceptus-maternal communication during maintenance and termination of pregnancy, including the role of species-specific decidualization. *Theriogenology* **150**: 329–338.

Kroll J, Waltenberger J. 1998. VEGF-A induces expression of eNOS and iNOS in endothelial cells via VEGF receptor-2 (KDR). Biochem Biophys Res Commun. **252**(3):743-6.

Kupper N, Huppertz B. 2022. The endogenous exposome of the pregnant mother: placental extracellular vesicles and their effect on the maternal system. *Mol Asp Med* **87.**

Kurbanov, B. 2018. The role of VEGF as prognostic marker of preeclampsia. *Pregnancy Hypertens* **13**: S68.

Lakhal S, Wood MJA. 2011. Exosome nanotechnology: an emerging paradigm shift in drug delivery: exploitation of exosome nanovesicles for systemic in vivo delivery of RNAi heralds new horizons for drug delivery across biological barriers. *BioEssays* **33**: 737–741.

Lal BK, Varma S, Pappas PJ, Hobson RW 2nd, Durán WN. 2001. VEGF increases permeability of the endothelial cell monolayer by activation of PKB/akt, endothelial nitric-oxide synthase, and MAP kinase pathways. *Microvasc Res* **62**(3): 252-62.

Landgraf P, Rusu M, Sheridan R, Sewer A, Iovino N, Aravin A, et al. 2007. A mammalian microRNA expression atlas based on small RNA library sequencing. *Cell* **129**(7):1401–1414.

Li H, Cao G, Zhang N, Lou T, Wang Q, Zhang Z, Liu C. 2018. RBP4 regulates trophoblastic cell proliferation and invasion via the PI3K/AKT signaling pathway. *Mol Med Rep* **18**: 2873–2879.

Li R, Wang N, Xue M, Long W, Cheng C, Mi C, Gao Z. 2019. A potential regulatory network among WDR86-AS1, miR-10b-3p, and LITAF is possibly involved in preeclampsia pathogenesis. *Cell Signal* **55**: 40–52.

Liu R, Liu J, Ji X, Liu Y. 2013. Synthetic nucleic acids delivered by exosomes: a potential therapeutic for generelated metabolic brain diseases. *Metab Brain Dis* **28**: 551–562.

Liu T, Zhang M, Mukosera GT, Borchardt D, Li Q, Tipple TE, Ishtiaq Ahmed AS, Power GG, Blood AB. 2019. L-NAME releases nitric oxide and potentiates subsequent nitroglycerin-mediated vasodilation. *Redox Biol* **26**: 101238.

Lok CAR, Van Der Post JAM, Sargent IL, Hau CM, Sturk A, Boer K, Nieuwland R. 2008. Changes in microparticle numbers and cellular origin during pregnancy and preeclampsia. *Hypertens Pregnancy* **27**: 344–360.

Loscalzo G, Scheel J, Ibañez-Cabellos JS, García-Lopez E, Gupta S, García-Gimenez JL, Mena-Mollá S, Perales-Marín A, Morales-Roselló J. 2021. Overexpression of microRNAs miR-25-3p, miR-185-5p and miR-132-3p in late onset fetal growth restriction, validation of results and study of the biochemical pathways involved. *Int J Mol Sci* **23**: 293.

Lv Y, Lu C, Ji X, Miao Z, Long W, Ding H, Lv M. 2019. Roles of microRNAs in preeclampsia. *J Cell Physiol* **234**: 1052–1061.

Makris A, Thornton C, Thompson J, et al. 2007. Uteroplacental ischemi a results in proteinuric hypertension and elevated sFLT-1. *Kidney Int* **71**: 977–984.

Mastorakos G, Ilias I. 2003. Maternal and fetal hypothalamic-pituitary-adrenal axes during pregnancy and postpartum. Ann N Y *Acad Sci* **997**: 136–149.

Mathiesen A, Hamilton T, Carter N, Brown M, McPheat W, Dobrian A. 2021. Endothelial extracellular vesicles: from keepers of health to messengers of disease. *Int J Mol Sci* **22**: 4640.

Mathivanan S, Lim JW, Tauro BJ, Ji H, Moritz RL, Simpson RJ. 2010. Proteomics analysis of A33 immunoaffinity-purified exosomes released from the human colon tumor cell line LIM1215 reveals a tissue-specific protein signature. Mol Cell Proteomics. **9**(2): 197–208.

Matsubara K. 2023. The potential for exosomes in the prevention and treatment of preeclampsia. *Hypertension Res in Preg* **3**:38-45.

Menon R, Debnath C, Lai A, Guanzon D, Bhatnagar S, Kshetrapal PK, Sheller-Miller S, Salomon C, Garbhini study team. 2019. Circulating exosomal miRNA profile during term and preterm birth pregnancies: a longitudinal study. *Endocrinology* **160**: 249–275.

Menon R, Mesiano S, Taylor RN. 2017. Programmed fetal membrane senescence and exosome-mediated signaling: a mechanism associated with timing of human parturition. *Front Endocrinol* **8**: 196.

Miller MJS, Thompson JH, Liu X, Eloby-Childress S, Sadowska-Krowicka, Zhang X-Jing, Clark DA. 1996. Failure of L-NAME to cause inhibition of nitric oxide synthesis: role of inducible nitric oxide synthase. *Inflamm Res* **45**: 272-276.

Mincheva-Nilsson L, Baranov V. 2014. Placenta-derived exosomes and syncytiotrophoblast microparticles and their role in human reproduction: immune modulation for pregnancy success. *Am J Reprod Immunol* **72**(5): 440–57.

Mitchell MD, Peiris HN, Kobayashi M, Koh YQ, Duncombe G, Illanes SE, Rice GE, Salomon C. 2015. Placental exosomes in normal and complicated pregnancy. *Am J Obstet Gynecol* **213** Suppl: S173–S181.

Miyagi Y, Koshikawa N, Yasumitsu H, Miyagi E, Hirahara F, Aoki I, Misugi K, Umeda M, Miyazaki K. 1994. cDNA cloning and mRNA expression of a serine proteinase inhibitor secreted by cancer cells: identification as placental protein 5 and tissue factor pathway inhibitor-2. *J Biochem* **116**: 939–942.

Miquerol L, Langille BL, Nagy A. 2000. Embryonic development is disrupted by modest increases in vascular endothelial growth factor gene expression. *Development* **127**(18): 3941-6.

Mochan S, Dhingra MK, Gupta SK, Saxena S, Arora P, Yadav V, Rani N, Luthra K, Dwivedi S, Bhatla N, Dhingra R. 2019. Status of VEGF in preeclampsia and its effect on endoplasmic reticulum stress in placental trophoblast cells. *Eur J Obstet Gynecol Reprod Biol X* **21**(4):100070.

Morales-Prieto DM, Chaiwangyen W, Ospina-Prieto S, Schneider U, Herrmann J, Gruhn B, et al. 2012. MicroRNA expression profiles of trophoblastic cells. *Placenta* **33**(9): 725–34.

Motta C, Grosso C, Zanuzzi C, Molinero D, Picco N, Bellingeri R, Alustiza F, Barbeito C, Vivas A, Romanini MC. 2015. Effect of sildenafil on pre-eclampsia-like mouse model induced by L-NAME. *Reprod in domestic animals* PMID25959785.

Murakami Y, Kobayashi T, Omatsu K, Suzuki M, Ohashi R, Matsuura T, Sugimura M, Kanayama N. 2005. Exogenous vascular endothelial growth factor can induce preeclampsia-like symptoms in pregnant mice. *Semin Thromb Hemost* **31**: 307–313.

Nair S, Salomon C. 2018. Extracellular vesicles and their immunomodulatory functions in pregnancy. *Semin Immunopathol* **40**: 425–437.

Nakahara A, Nair S, Ormazabal V, Elfeky O, Garvey C. E, Longo S, et al. 2020. Circulating placental extracellular vesicles and their potential roles during pregnancy. *Ochsner J* **20**: 439–445.

Napso T, Yong HEJ, Lopez-Tello J, Sferruzzi-Perri AN. 2018. The role of placental hormones in mediating maternal adaptations to support pregnancy and lactation. *Front Physiol* **9**: 1091.

Nguyen SL, Greenberg JW, Wang H, Collaer BW, Wang J, Petroff MG. 2019. Quantifying murine placental extracellular vesicles across gestation and in preterm birth data with tidyNano: a computational framework for analyzing and visualizing nanoparticle data in R. *PLoS One* **14**: e0218270.

North RA, Ferrier C, Long D, Townend K, Kincaid-Smith P. 1994. Uterine artery Doppler flow velocity waveforms in the second trimester for the prediction of preeclampsia and fetal growth retardation. *Obstet Gynecol* **83**: 378–386.

Nowak M, Gram A, Boos A, Aslan S, Ay SS, Önyay F, Kowalewski MP. 2017. Functional implications of the utero-placental relaxin (RLN) system in the dog throughout pregnancy and at term. *Reproduction* **154**: 415–431.

Outhwaite JE, McGuire V, Simmons DG. 2015. Genetic ablation of placental sinusoidal trophoblast giant cells causes fetal growth restriction and embryonic lethality. *Placenta* **36**(8): 951-955.

Pfeiffer S, Leopold E, Schmidt K, Brunner F, Mayer B. 1996. Inhibition of nitric oxide synthesis by NG-nitro-L-arginine methyl ester (L-NAME): requirement for bioactivation to the free acid, NG-nitro-L-arginine. *Br J Pharmacol* **118**: 1433–1440.

Pillay P, Maharaj N, Moodley J, Mackraj I. 2016. Placental exosomes and pre-eclampsia: Maternal circulating levels in normal pregnancies and, early and late onset pre-eclamptic pregnancies. *Placenta* **46**: 18–25.

Pollheimer J, Knöfler M. 2012. The role of the invasive, placental trophoblast in human pregnancy. *Wien Med Wochenschr* **162**: 187–190.

Popiel-Kopaczyk A, Grzegrzolka J, Piotrowska A, Olbromski M, Smolarz B, Romanowicz H, Rusak A, Mrozowska M, Dziegiel P, Podhorska-Okolow M and Kobierzycki C. 2023. The expression of Testin, Ki-67 and p16 in cervical cancer diagnostics. *Curr Issues Mol Biol* **45**: 490–500.

Purcell T, Buhimschi I, Given R, Chwalisz K, Garfield R. 1997. Inducible nitric oxide synthase is present in the rat placenta at the fetal-maternal interface and decreases prior to labour. *Mol human reprod* **3**: 485-91.

Rajaratnam N, Ditlevsen NE, Sloth JK, Baek R, Jorgensen MM, Christiansen OB. 2021. Extracellular vesicles: an important biomarker in recurrent pregnancy loss? *J Clin Med* **10**(12): 2549.

Ramanlal R, Gupta V. 2023. Physiology, vasodilation. In: StatPearls [Internet]. Treasure Island (FL): StatPearls Publishing. PMID: 32491494.

Raposo G, Stoorvogel W. 2013. Extracellular vesicles: exosomes, microvesicles, and friends. *J Cell Biol* **200**: 373–383.

Ricard N, Bailly S, Guignabert C, Simons M. 2021. The quiescent endothelium: signaling pathways regulating organ-specific endothelial normalcy. *Nat Rev Cardiol* **18**: 565–580.

Rivas MA, Venturutti L, Huang YW, Schillaci R, Huang TH, Elizalde PV. 2012. Downregulation of the tumor-suppressor miR-16 via progestin-mediated oncogenic signaling contributes to breast cancer development. B*reast Cancer Res* **14**(3): R77.

Roberts JM, Taylor RN, Musci TJ, Rodgers GM, Hubel CA, McLaughlin MK. 1989. Preeclampsia: an endothelial cell disorder. *Am J Obs Gynecol* **161**:1200–1204.

Rocha FG, Slavin TP, Li D, Tiirikainen MI, Bryant-Greenwood GD. 2013. Genetic associations of relaxin: preterm birth and premature rupture of fetal membranes. *Am J Obstet Gynecol* **209**: 258.e1–258.e8.

Runyan CL, McIntosh SZ, Maestas MM, Quinn KE, Boren BP, Ashley RL. 2019. CXCR4 signaling at the ovine fetal-maternal interface regulates vascularization, CD34+ cell presence, and autophagy in the endometrium. *Biol Reprod* **101**: 102–111.

Salomon C, Kobayashi M, Ashman K, Sobrevia L, Mitchell MD, Rice GE. 2013. Hypoxia-induced changes in the bioactivity of cytotrophoblast derived exosomes. *PLoS One* **8**: e79636.

Salomon C, Torres MJ, Kobayashi M, Scholz-Romero K, Sobrevia L, Dobierzewska A, et al. 2014. A gestational profile of placental exosomes in maternal plasma and their effects on endothelial cell migration. *PloS one* **9**(6): e98667.

Salomon C, Guanzon D, Scholz-Romero K, et al. 2017. Placental Exosomes as Early Biomarker of Preeclampsia: Potential Role of Exosomal MicroRNAs Across Gestation. *J Clin Endocrinol Metab* **102**(9): 3182–3194.

Santiago-Sánchez GS, Pita-Grisanti V, Quiñones-Díaz B, Gumpper K, Cruz-Monserrate Z, Vivas-Mejía PE. 2020. Biological functions and therapeutic potential of lipocalin 2 in cancer. *Int J Mol Sci* **21**: 4365.

Sarker S, Scholz-Romero K, Perez A, Illanes SE, Mitchell MD, Rice GE, Salomon C. 2014. Placenta-derived exosomes continuously increase in maternal circulation over the first trimester of pregnancy. *J Transl Med* **12**: 204.

Shang W, Wang Z. 2017. The update of NGAL in acute kidney injury. *Curr Protein Pept Sci* **18**: 1211–1217.

Shao C, Yang F, Miao S, et al. 2018. Role of hypoxia-induced exosomes in tumor biology. *Mol Cancer* **17**: 120.

Sheller-Miller S, Choi K, Choi C, Menon R. 2019a. Cyclic-recombinase-reporter mouse model to determine exosome communication and function during pregnancy. *Am J Obstet Gynecol* **221**: 502.e1–502.e12.

Sheller-Miller S, Trivedi J, Yellon SM, Menon R. 2019b. Exosomes cause preterm birth in mice: evidence for paracrine signaling in pregnancy. *Sci Rep* **9**: 608.

Simmons DG, Rawn S, Davies A, Hughes M, Cross JC. 2008. Spatial and temporal expression of the 23 murine prolactin/placental lactogen-related genes is not associated with their position in the locus. *BMC Genomics* **9**: 352

Skynner MJ, Drage DJ, Dean WL, Turner S, Watt DJ, Allen ND. 1999. Transgenic mice ubiquitously expressing human placental alkaline phosphatase (PLAP): an additional reporter gene for use in tandem with beta-galactosidase (lacZ). *Int J Dev Biol* **43**(1):85–90.

Smith TPL, Fahrenkrug SC, Rohrer GA, Simmen FA, Rexroad CE III, Keele JW. 2001. Mapping of expressed sequence tags from a porcine early embryonic cDNA library. *Anim Genet* **32**: 66–72.

Soncin F, Natale D, Parast MM. 2015. Signaling pathways in mouse and human trophoblast differentiation: a comparative review. *Cell Mol Life Sci* **72**: 1291-1302.

Steegers EA, von Dadelszen P, Duvekot JJ, Pijnenborg R. 2010. Pre-eclampsia. *Lancet* **376**(9741): 631-44.

Steinetz BG, Goldsmith LT, Lust G. 1987. Plasma relaxin levels in pregnant and lactating dogs. *Biol Reprod* **37**: 719–725.

Stenqvist AC, Nagaeva O, Baranov V, Mincheva-Nilsson L. 2013. Exosomes secreted by human placenta carry functional Fas ligand and TRAIL molecules and convey apoptosis in activated immune cells, suggesting exosome-mediated immune privilege of the fetus. *J Immunol* **191**: 5515–5523.

Stefanski AL, Martinez N, Peterson LK, Callahan TJ, Treacy E, Luck M, Friend SF, Hermesch A, Maltepe E, Phang T, Dragone LL, Winn VD. 2019. Murine trophoblast-derived and pregnancy-associated exosome-enriched extracellular vesicle microRNAs: Implications for placenta driven effects on maternal physiology. *PLoS One* **14**(2): e0210675.

Steven D. 1975. Anatomy of the placental barrier. In: Comparative placentation. Essays in structure and function, American Press. pp. 25-57.

Tadesse S, Luo G, Park JS, Kim BJ, Snegovskikh VV, Zheng T, Hodgson EJ, Arcuri F, Toti P, Parikh CR, Guller S, Norwitz ER. 2011. Intra-amniotic infection upregulates neutrophil gelatinase-associated lipocalin (NGAL) expression at the maternal-fetal interface at term: implications for infectionrelated preterm birth. *Reprod Sci* **18**: 713–722.

Tognoli ML, Dancourt J, Bonsergent E, Palmulli R, de Jong OG, Van Niel G, Rubinstein E, Vader P, Lavieu G. 2023. Lack of involvement of CD63 and CD9 tetraspanins in the extracellular vesicle content delivery process. *Commun Biol* **6**: 532.

Tkach M, Théry C. 2016. Communication by extracellular vesicles: where we are and where we need to go. *Cell* **164**: 1226–1232.

Udagawa K, Yasumitsu H, Esaki M, Sawada H, Nagashima Y, Aoki I, Jin M, Miyagi E, Nakazawa T, Hirahara F, Miyazaki K, Miyagi Y. 2002. Relaxin stimulates expression of vascular endothelial growth factor in normal human endometrial cells in vitro and is associated with menometrorrhagia in women. *Hum Reprod* **14**: 800–806.

Unemori EN, Erikson ME, Rocco SE, Sutherland KM, Parsell DA, Mak J, Grove BH. 1999. Subcellular localization of PP5/TFPI-2 in human placenta: a possible role of PP5/TFPI-2 as an anti-coagulant on the surface of syncytiotrophoblasts. *Placenta* **23**: 145–153.

Valadi H, Ekstrom K, Bossios A, Sjostrand M, Lee JJ, Lotvall JO. 2007. Exosome-mediated transfer of mRNAs and microRNAs is a novel mechanism of genetic exchange between cells. *Nat Cell Biol* **9**(6): 654–9.

Vargas A, Zhou S, Éthier-Chiasson M, Flipo D, Lafond J, Gilbert C, Barbeau B. 2014. Syncytin proteins incorporated in placenta exosomes are important for cell uptake and show variation in abundance in serum exosomes from patients with preeclampsia. *FASEB J* **28**: 3703–3719.

Vallhov H, Gutzeit C, Johansson SM, Nagy N, Paul M, Li Q, Friend S, George TC, Klein E, Scheynius A, Gabrielsson S. 2011. Exosomes containing glycoprotein 350 released by EBV-transformed B cells selectively target B cells through CD21 and block EBV infection in vitro. *J Immunol* **186**: 73–82.

van der Pol E, Coumans FA, Grootemaat AE, Gardiner C, Sargent IL, Harrison P, Sturk A, van Leeuwen TG, Nieuwland R. 2014. Particle size distribution of exosomes and microvesicles determined by transmission electron microscopy, flow cytometry, nanoparticle tracking analysis, and resistive pulse sensing. *J Thromb Haemost* **12**: 1182–1192.

van der Zee R, Murohara T, Luo Z, Zollmann F, Passeri J, Lekutat C, Isner JM. 1997. Vascular endothelial growth factor/vascular permeability factor augments nitric oxide release from quiescent rabbit and human vascular endothelium. *Circulation* **95**(4): 1030-1037.

van Niel G, D'Angelo G, Raposo G. 2018. Shedding light on the cell biology of extracellular vesicles. *Nat Rev Mol Cell Biol* **19**: 213–228.

Velegrakis A, Sfakiotaki M, Sifakis S. 2017. Human placental growth hormone in normal and abnormal fetal growth. *Biomed Rep* **7**: 115–122.

Wang L, Zhang W, Zou N, Zhang L. 2021. Trophoblasts modulate the Ca2+ oscillation and contraction of myometrial smooth muscle cells by small extracellular vesicle- (sEV-) mediated exporting of miR-25-3p during premature labor. *Oxid Med Cell Longev* **2021**: 8140667.

Wang Y, Fan H, Zhao G, Liu D, Du L, Wang Z, et al. 2012. MiR-16 inhibits the proliferation and angiogenesis-regulating potential of mesenchymal stem cells in severe pre-eclampsia. *FEBS J* **279**: 4510–4524

Wei W, Ao Q, Wang X, Cao Y, Liu Y, Zheng SG, Tian X. 2021. Mesenchymal stem cell-derived exosomes: a promising biological tool in nanomedicine. *Front Pharmacol* **25**(11): 590470.

Weisz A, Cicatiello L, Esumi H. 1996. Regulation of the mouse inducible-type nitric oxide synthase gene promoter by interferon-gamma, bacterial lipopolysaccharide and NG-monomethyl-L-arginine. *Biochem J* **15**(316): 209-215.

Williams KC, Renthal NE, Condon JC, Gerard RD, Mendelson CR. 2012. MicroRNA-200a serves a key role in the decline of progesterone receptor function leading to term and preterm labor. *Proc Natl Acad Sci USA* **109**: 7529–7534.

Witvrouwen I, Gevaert AB, Possemiers N, Ectors B, Stoop T, Goovaerts I, Boeren E, Hens W, Beckers PJ, Vorlat A, Heidbuchel H, Van Craenenbroeck AH, Van Craenenbroeck EM. 2021. Plasma-derived microRNAs are influenced by acute and chronic exercise in patients with heart failure with reduced ejection fraction. *Front Physiol* **27**(12): 736494.

Yáñez-Mó M, Siljander PRM, Andreu Z, Zavec AB, Borràs FE, Buzas EI, Buzas K, Casal E, Cappello F, Carvalho J, Colás E, Cordeiro-da Silva A, Fais S, Falcon-Perez JM, Ghobrial IM, Giebel B, Gimona M, Graner M, Gursel I, Gursel M, Heegaard NHH, Hendrix A, Kierulf P, Kokubun K, Kosanovic M, Kralj-Iglic V, Krämer-Albers EM, Laitinen S, Lässer C, Lener T, Ligeti E, Linē A, Lipps G, Llorente A, Lötvall J, Manček-Keber M, Marcilla A, Mittelbrunn M, Nazarenko I, Nolte-'t Hoen ENM, Nyman TA, O'Driscoll L, Olivan M, Oliveira C, Pállinger É, Del Portillo HA, Reventós J, Rigau M, Rohde E, Sammar M, Sánchez-Madrid F, Santarém N, Schallmoser K, Ostenfeld MS, Stoorvogel W, Stukelj R, Van der Grein SG, Vasconcelos MH, Wauben MHM, De Wever O. 2015. Biological properties of extracellular vesicles and their physiological functions. *J Extracell Vesicles* **4**: 27066.

Yang H, Ma Q, Wang Y, Tang Z. 2020. Clinical application of exosomes and circulating microRNAs in the diagnosis of pregnancy complications and foetal abnormalities. *J Transl Med* **18**:1–9.

Yoshikawa K, Umekawa T, Maki S, Kubo M, Nii M, Tanaka K, Tanaka H, Osato K, Kamimoto Y, Kondo E, et al. 2017 Tadalafil improves L-NG-nitroarginine methyl ester-induced preeclampsia with fetal growth restriction-like symptoms in pregnant mice. *Am J Hypertens* **31**: 89–96.

Yoshioka Y, Konishi Y, Kosaka N, Katsuda T, Kato T, Ochiya T. 2013. Comparative marker analysis of extracellular vesicles in different human cancer types. *J Extracell Vesicles* **2**: 20424.

Yustinasari LR, Kuratomi M, Kagawa S, Gondo A, Aramaki N, Imai H, Kusakabe KT. 2024. Specific expression and blood kinetics for relaxin 2, lipocalin 2, and tissue factor pathway inhibitor 2 at the canine placenta and pregnant bloods. *J Vet Med Sci* **86**(1): 77-86.

Zaborowski MP, Balaj L, Breakefield XO and Lai CP. 2015. Extracellular vesicles: composition, biological relevance, and methods of study. *Bioscience* **65**: 783–797.

Zhang H, Freitas D, Kim HS, Fabijanic K, Li Z, Chen H, Mark MT, Molina H, Martin AB, Bojmar L, Fang J, Rampersaud S, Hoshino A, Matei I, Kenific CM, Nakajima M, Mutvei AP, Sansone P, Buehring W, Wang H, Jimenez JP, Cohen-Gould L, Paknejad N, Brendel M, Manova-Todorova K, Magalhães A, Ferreira JA, Osório H, Silva AM, Massey A, Cubillos-Ruiz JR, Galletti G, Giannakakou P, Cuervo AM, Blenis J, Schwartz R, Brady

MS, Peinado H, Bromberg J, Matsui H, Reis CA, Lyden D. 2018. Identification of distinct nanoparticles and subsets of extracellular vesicles by asymmetric flow field-flow fractionation. *Nat Cell Biol* **20**: 332–343.

Zhang ZG, Chopp M. 2016. Exosomes in stroke pathogenesis and therapy. *J Clin Invest* **126**: 1190–1197.

Zhang J., Li H., Fan B., Xu W., Zhang X. 2020. Extracellular vesicles in normal pregnancy and pregnancy-related diseases. *J Cell Mol Med* **24**: 4377–4388.

Zhang JT, Cai QY, Ji SS, Zhang HX, Wang YH, Yan HT, Yang XJ. 2016. Decreased miR-143 and increased miR-21 placental expression levels are associated with macrosomia. *Mol Med Rep* **13**: 3273–3280.

Zheng L, Huang J, Su Y, Wang F, Kong H, Xin H. 2020. Overexpression of tissue factor pathway inhibitor 2 attenuates trophoblast proliferation and invasion in preeclampsia. *Hum Cell* **33**: 512–520.

Zhou D, Qu B, Zhang X. 2022. Diagnostic value of serum miR-25-3p in hypertensive disorders in pregnancy. *Women Health* **62**: 818–826.

Zhu X, Han T, Sargent II, Yin G, Yao Y. 2009. Differential expression profile of microRNAs in human placentas from preeclamptic pregnancies vs normal pregnancies. *Am J Obstet Gynecol* **200**: 661.e1-661.e7.

Zhu Y, Lu H, Huo Z, Ma Z, Dang J, Dang W, et al. 2016. MicroRNA-16 inhibits feto-maternal angiogenesis and causes recurrent spontaneous abortion by targeting vascular endothelial growth factor. *Sci Rep* **6**: 35536.

SUMMARY

Studies of exosome dynamics in mice and canines during normal pregnancy and the roles of exosomes and microRNA in the pathogenesis of preeclampsia

This dissertation examines the role of exosomes in the serum of pregnant mammals. The concentration of exosomes typically increases during gestation in mice, but there are no changes in canines. Overall, this study was conducted to confirm the specific genes in the placenta, their corresponding translation proteins in the serum, and to detect whether cell-free RNA is present in serum-derived extracellular vesicles (EVs). Furthermore, this study observed the expression of tetraspanin surface proteins, commonly used as markers for EVs, in relation to the exosome concentration detected by nanoparticle tracking analysis (NTA). Since there is no specific marker for exosomes, multiple methods, including western blot and immunohistochemistry, were used to prove the existence of EVs. These methods are essential for detecting exosomes in the serum and placenta. Despite differences in exosome concentration between normal and abnormal pregnancies, the study suggests that miRNA packed in exosomes may play a role in the pathophysiology of normal pregnancy and the development of diseases such as preeclampsia.

The first study examined specific genes found in canine placentas and their corresponding protein expression in serum during pregnancy. The research involved sequencing placental RNA and identifying three out of 15 top genes as specific placental genes, namely lipocalin 2, relaxin 2, and tissue factor pathway inhibitor 2. To investigate their expression in serum during different stages of pregnancy, reverse-transcription PCR and western blotting were performed. While the concentration of exosomes during canine pregnancy did not significantly increase, the successful detection of cell-free RNA related to relaxin 2 suggests the potential for specific marker genes. This indicates that factors contained in exosomes may still be present and reflect fetal development and placental formation in pregnant canine serum.

In the second study, we conducted research on mice pregnancy. Our findings demonstrated that among tetraspanin surface protein markers, CD63 shows a similar expression pattern to the exosome concentration isolated from serum at each stage of pregnancy as shown by NTA. This study suggests that exosomes containing miRNAs, particularly miR-10b-3p, miR-25b-3p, and miR-143-3p, play an important role in normal pregnancy, especially on Gd 18.5, just before parturition. Additionally, using anti-CD63, this study described the localization of exosomes in the mouse placenta for the first time.

The third study was a follow-up to the second study, which used mouse models to study preeclampsia. In order to create a preeclamptic condition in the mice, L-N^G-Nitro-arginine methyl ester (L-NAME) was injected to raise their blood pressure and induce proteinuria. The study found increased levels of vascular endothelial growth factor (VEGF) and inducible nitric oxide synthase (iNOS) proteins in the serum-derived EVs and placental tissue of the preeclamptic mice. Additionally, the total concentration of exosomes in the serum was higher in the preeclampsia mouse model, and there was a decrease in miR-16-5p and an increase in miR-25b-3p. It is believed that the low expression of miR-16-5p may lead to inflammation and increased VEGF levels, potentially contributing to the development of preeclampsia.

Finally, this dissertation concluded that exosomes derived from serum, which are expected to originate from the placenta, play a role in the normal progression of pregnancy as well as in the development of preeclampsia. The study found a relationship between the quantity and content of exosomes and placental dysfunction in a preeclampsia mouse model induced by L-NAME. Different levels of exosomal miRNA were found to be linked to these pathological conditions. Therefore, changes in the release of exosomes, their concentration, composition, and bioactivity are associated with pregnancy complications. Additionally, targeting exosomal miRNAs and related pathways may have great potential for the treatment of preeclampsia.